SDE-driven modeling of phenotypically heterogeneous tumors: The influence of cancer cell stemness

Julia M. Kroos
Basque Center for Applied Mathematics, Alameda Mazarredo 14,
48009 Bilbao, Spain

Christian Stinner
Technische Universität Darmstadt, Schlossgartenstr. 7,
64289 Darmstadt, Germany

Christina Surulescu*
Technische Universität Kaiserslautern, Felix-Klein-Zentrum für Mathematik,
Paul-Ehrlich-Str. 31, 67663 Kaiserslautern, Germany

Nico Surulescu
German Breast Group Forschungs GmbH, Martin-Behaim-Str. 12,
63263 Neu-Isenburg, Germany

Thursday 23rd May, 2019

Abstract

We deduce cell population models describing the evolution of a tumor (possibly interacting with its environment of healthy cells) with the aid of differential equations. Thereby, different subpopulations of cancer cells allow accounting for the tumor heterogeneity. In our settings these include cancer stem cells known to be less sensitive to treatment and differentiated cancer cells having a higher sensitivity towards chemo- and radiotherapy. Our approach relies on stochastic differential equations in order to account for randomness in the system, arising e.g., due to the therapy-induced decreasing number of clonogens, which renders a pure deterministic model arguable. The equations are deduced relying on transition probabilities characterizing innovations of the two cancer cell subpopulations, and similarly extended to also account for the evolution of normal tissue. Several therapy approaches are introduced and compared by way of tumor control probability (TCP) and uncomplicated tumor control probability (UTCP). A PDE approach allows to assess the evolution of tumor and normal tissue with respect to time and to cell population densities which can vary continuously in a given set of states. Analytical approximations of solutions to the obtained PDE system are provided as well.

1 Introduction

Phenotypic and functional tumor heterogeneity is an important feature of neoplastic lesions. During the last decade there has been increasing evidence that a subpopulation of cancer cells exhibiting the characteristics of stem cells triggers the initiation and growth of the tumor, also playing an essential role in metastasis, see e.g., [60] and references therein. According to the cancer stem cell hypothesis, tumors are initiated and sustained by a small subset of cancer cells with the abilities of self-renewal and production of differentiated cells of diverse lineages [66]. Depending on the biochemical conditions in the tumor microenvironment, cancer stem cells (CSCs) can undergo several types of mitosis (see e.g., [12]): symmetric self-renewal, when both daughter cells keep the characteristics of stem cells; asymmetric self-renewal, when only one of the daughter cells stays a stem cell, while the other becomes a progenitor cell; and division into two progenitor cells. Progenitor cells have intermediate properties between stem cells and differentiated cells; they can divide symmetrically or unsymmetrically, undergoing self-renewal, or yielding two differentiated daughter cells. While differentiated (progenitor) cells are relatively short-lived,

*surulescu@mathematik.uni-kl.de

having a limited mitotic potential, cancer stem cells seem to have acquired a limitless replicative potential or immortality [25], thus they are able to persist long enough to accomplish oncogenic mutations and to migrate and establish new tumors at distal sites in the body. Moreover, cancer stem cells are suspected to be responsible for the recurrence of the disease after treatment [47, 55]. This is thought to be due to some cancer cells evolving with the capacity of resistance to chemo and/or radiotherapy [3, 37]. Therefore, therapies specifically targeting cancer stem cells are likely to be a critical determinant in achieving complete tumor eradication, see [9] and references therein; we also refer to [13] for a mathematical model addressing this issue.

A large palette of mathematical models for various aspects of CSC dynamics has been proposed. They range from deterministic compartmental models involving several types of cells in different stages and formulated in an ODE framework, see, e.g., [5, 13, 21, 63] to models accounting for spatial effects, possibly also under the influence of the tumor microenvironment in a discrete, agent-based [17, 16] or continuous [18, 68] manner. Models also accounting for random effects via transition probabilities [24, 64], stochastic processes [19], or stochastic differential equations [52] have been proposed as well, however not all of them considering stemness or phenotype heterogeneity of the cancer cells. Some of the models mentioned above also relate to the influence of CSC dynamics on chemo and/or radiotherapy response. While including randomness in the models describing the therapy-free evolution of CSCs in interaction with differentiated cells (DCs) and normal tissue accounts e.g., for perturbations in the tumor microenvironment reflecting on the cell population, for cell-to-cell variations or for differences in the cell cycle stage, in the context of therapy stochasticity becomes a desirable feature of the mathematical settings: By therapeutical interventions the number of clonogens is supposed to be drastically reduced (up to eradication), which makes a purely deterministic model questionable. Models involving CSCs and assessing some kind of applied treatment while explicitly accounting for stochasticity are rarer: For instance, in [58] the authors use birth-death Markov chains in continuous time to investigate the extinction times of cancer stem cells and normal stem cells; [39] also used a continuous time, discrete state-space birth-death process. Iwasa et al. [31] developed a model for acquired drug resistance and determined the resistance probability of an exponentially growing cell population starting from one sensitive cell and reaching a given detection size and found that a tumor subject to high rates of apoptosis will show a higher incidence of resistance than expected on its detection size only. Fakir et al. [19] considered a stochastic tumor control probability (TCP)[1] model incorporating repopulation of stem-like cancer cells and their mutual interactions within microenvironmental niches. The TCP is computed upon relying on probability distributions of a prespecified shape and corresponding survival and repopulation matrices involving niche-endogenous birth and death rates. Continuum SDE models for the evolution of tumor cells offer a way to account for intrinsic and extrinsic uncertainties in connection to CSCs and their interactions with DCs and normal tissue. SDE models used in the context of cancer growth and assessing the TCP and the probability distributions of times to extinction for the considered populations of cancer cells were proposed in [65] and later in [40].

In this work we introduce a class of SDE models describing the interplay between CSCs and tumor DCs. Their formal deduction is presented in Section 2 and follows the method proposed by Allen, see e.g., [2], and also used in a first form in [40]. However, an essential modification is done here in order to ensure non-negativity of the solutions. The restrictions imposed by the latter actually guide the modeling in this framework. For these models we perform numerical simulations in order to illustrate the (pathways and averaged) behavior of the two subpopulations of interacting cancer cells. In Section 3 we extend the settings to account for therapy, thereby looking both at a time-discrete approach and its continuous counterparts. Several different treatment schedules involving chemo and/or radiotherapy are considered. Section 4 is dedicated to assessing the various treatment strategies applied to the DCs and CSC populations. The subsequent Section 5 proposes a model version supplementary accommodating the dynamics of the normal cells. For the new model we evaluate in Section 6 the therapy effects on normal cells with the aid of the normal tissue complication probability (NTCP) and the overall treatment efficacy by way of the uncomplicated tumor control probability (UTCP). Section 7 provides a PDE approach to assessing the future evolution (in the mean) of the tumor and normal tissue based on the tumor state known at some given moment of time. Such prediction of the tumor evolution is of high relevance for the patients and for clinical trials, as it helps to estimate and compare the disease evolution under diverse classes of a tumor staging system or different treatments. Thereby, the quantities of interest here are expectations of the total tumor burden, its stemness portion, and the deviation of normal tissue from a critical functionality threshold. A way to derive analytical approximations in closed-form

[1] The TCP gives the probability that no clonogenic cells survive the treatment.

for such quantities is also presented. The method can be extended to predict other interesting future numerical characteristics of the tumor (e.g., its standard deviation or survival probabilities for some given thresholds). Moreover, the proposed PDE approach is less time consuming and numerically more efficient than the standard one based on simulating the SDE system. We deduce the corresponding linear and nonautonomous PDEs, solve them numerically, and also provide analytical approximations of the solution components. Finally, in Section 8 we provide some comments on the perspectives of our modeling approach.

2 An SDE model for a heterogeneous tumor without treatment

2.1 Model setup

We derive an SDE model for the differentiated cancer cells and the cancer stem cells. To this aim, let $c(t)$ and $s(t)$ denote the population sizes of the former and of the latter, respectively, at time t. We want to analyze the interactions between these two populations and are going to proceed as in [2]. We make the following assumptions (see also [27]):

1. Cancer stem cells are immortal and have unlimited replicative potential, see e.g. [44] and references therein.

2. As mentioned in Section 1, each of the cancer stem cells is able to divide in various ways; for simplicity, we assimilate in the respective subpopulation progenitor to differentiated cells:

   - into two stem cells (with probability a_1),
   - into one differentiated cancer cell and one cancer stem cell (with probability a_2) or
   - into two differentiated cancer cells (with probability a_3)

   with $a_i \in [0,1]$ for $i = 1,2,3$ and $\sum_{i=1}^{3} a_i = 1$.
   The probabilities a_i are commonly chosen to be constants, however in order to ensure the non-negativity of solutions to our model (1) below, we will require a_2 and a_3 to be proportional to the density c of differentiated cancer cells. Indeed, there is evidence of the latter influencing the CSC dynamics and their properties [45, 57]. We postulate that the differentiation of CSCs into DCs is favored by the two phenotypes being in contact (while the direct birth and death of either phenotype are not influenced by other processes) and choose here

   $$a_i(c) = \frac{\widetilde{a_i} c}{\widetilde{a_1} + \widetilde{a_2} c + \widetilde{a_3} c}, \quad i = 2,3, \qquad a_1(c) = \frac{\widetilde{a_1}}{\widetilde{a_1} + \widetilde{a_2} c + \widetilde{a_3} c}$$

   with $\widetilde{a_i}$ being positive constants. Other choices are possible as well, the only restriction being that $a_i(0) = 0$ for $i = 2,3$ and $\sum_{i=1}^{3} a_i(c) = 1$. Moreover, as in previous models, e.g. [11, 26, 27] we assume the differentiation process to be irreversible.

3. Differentiated cancer cells are mortal and have a finite potential to divide.

4. During proliferation differentiated cancer cells divide into two cells, each of them being again a differentiated cancer cell.

The relevant occurrences in connection with the differentiated and stem cell dynamics in a tumor can be described schematically as in Figure 1.
The parameters used above have the following meaning: b_c: proliferation rate of c-cells (symmetric differentiation only); b_s: proliferation rate of stem cells (with the three possibilities enumerated in 2. above), and d_s, d_c: death rates.

The above assumptions lead to $b_s, d_c > 0$, $d_s \geq 0$, $b_c = 0$[2]. For a small interval of time of legth Δt (such that the envisaged changes happen independently of each other; in particular we also assume that

[2] Actually, b_c becomes negligible after a few differentiations; in order to simplify the computations we directly assume $b_c = 0$, see also [27]. The stem cells are practically immortal (see our first assumption above), thus we could set $d_s = 0$. In Section 3, however, we will also take into account death rates which are not inherent to the population, but are due to treatment application, hence there a death rate $d_s > 0$ will be considered.

differentiation events do not happen simultaneously to birth and death in the s-population) we register in Table 1 the respective transition probabilities for $\mathbf{X} = (c, s)^t$, upon relying on the scheme in Figure 1.

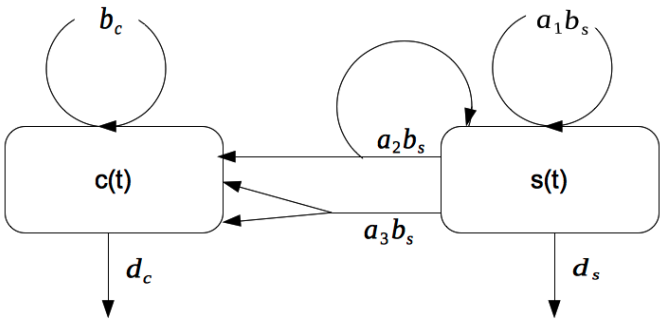

Figure 1: Interaction of differentiated cancer cells c and cancer stem cells s.

Changes in X	**Probability**
$\Delta X^{(1)} = (1,0)^t$	$p_1 = a_2(c)b_s s\Delta t$
$\Delta X^{(2)} = (-1,0)^t$	$p_2 = d_c c\Delta t$
$\Delta X^{(3)} = (0,1)^t$	$p_3 = a_1(c)b_s s\Delta t$
$\Delta X^{(4)} = (0,-1)^t$	$p_4 = d_s s\Delta t$
$\Delta X^{(5)} = (2,-1)^t$	$p_5 = a_3(c)b_s s\Delta t$
$\Delta X^{(6)} = (-1,1)^t$	$p_6 = d_c c a_1(c)b_s s\Delta t$
$\Delta X^{(7)} = (2,0)^t$	$p_7 = 0$
$\Delta X^{(8)} = (-1,-1)^t$	$p_8 = d_c c d_s s\Delta t$
$\Delta X^{(9)} = (1,-1)^t$	$p_9 = b_c c d_s s\Delta t = 0$
$\Delta X^{(10)} = (1,1)^t$	$p_{10} = b_c c a_1(c)b_s s\Delta t = 0$
$\Delta X^{(11)} = (3,-1)^t$	$p_{11} = 0$
$\Delta X^{(12)} = (0,0)^t$	$p_{12} = 1 - \sum_{i=1}^{11} p_i$

Table 1: Transition probabilities for $\mathbf{X} = (c, s)^t$, according to the scheme in Figure 1.

Then at a given time t the expectation and the covariance matrix are:

$$\mathbb{E}(\Delta\mathbf{X}) = \sum_{i=1}^{12} p_i \Delta X^{(i)} = \begin{pmatrix} (a_2(c(t)) + 2a_3(c(t)))b_s s(t) - (a_1(c(t))b_s + d_s)d_c c(t)s(t) - d_c c(t) \\ (a_1(c(t)) - a_3(c(t)))b_s s(t) + (a_1(c(t))b_s - d_s)d_c c(t)s(t) - d_s s(t) \end{pmatrix} \Delta t$$

$$\mathbb{E}\left(\Delta\mathbf{X}(\Delta\mathbf{X})^t\right) = \sum_{i=1}^{12} p_i \Delta X^{(i)} \left(\Delta X^{(i)}\right)^t =: \begin{pmatrix} u & v \\ v & w \end{pmatrix} \Delta t,$$

with

$$\begin{aligned} u &= d_c c(t) + (a_2(c(t)) + 4a_3(c(t)))b_s s(t) + (d_s + a_1(c(t))b_s)d_c c(t)s(t), \\ v &= -2a_3(c(t))b_s s(t) + (d_s - a_1(c(t))b_s)d_c c(t)s(t) \\ w &= d_s s(t) + (a_1(c(t)) + a_3(c(t)))b_s s(t) + (d_s + a_1(c(t))b_s)d_c c(t)s(t). \end{aligned}$$

It is straightforward to show that

$$\mathbb{V} := \frac{\mathbb{E}\left(\Delta\mathbf{X}(\Delta\mathbf{X})^t\right)}{\Delta t}$$

is positive-definite. Hence the square root of the matrix $\mathbb{V}$ exists and we denote it by $\mathbb{B} := \mathbb{V}^{1/2}$. Further we define and compute:

$$\boldsymbol{\mu} := \frac{\mathbb{E}(\Delta\mathbf{X})}{\Delta t} = \begin{pmatrix} (a_2(c(t)) + 2a_3(c(t)))b_s s(t) - (a_1(c(t))b_s + d_s)d_c c(t)s(t) - d_c c(t) \\ (a_1(c(t)) - a_3(c(t)))b_s s(t) + (a_1(c(t))b_s - d_s)d_c c(t)s(t) - d_s s(t) \end{pmatrix},$$

$$\mathbb{V} \;:=\; \frac{\mathbb{E}\,(\Delta\mathbf{X}(\Delta\mathbf{X})^t)}{\Delta t} = \begin{pmatrix} u & v \\ v & w \end{pmatrix}.$$

The matrix $\mathbb{B}$ can be explicitly computed (see e.g., [2]):

$$\mathbb{B} \;=\; \mathbb{V}^{1/2} = \begin{pmatrix} u & v \\ v & w \end{pmatrix}^{1/2} = \frac{1}{\eta}\begin{pmatrix} u+\tau & v \\ v & w+\tau \end{pmatrix}$$

with $\tau = \sqrt{uw - v^2}$ and $\eta = \sqrt{u + w + 2\tau}$. The system of stochastic differential equations for the dynamics of the two cancer cell populations is then given by

$$d\mathbf{X} = \boldsymbol{\mu}(\mathbf{X})dt + \mathbb{B}(\mathbf{X})d\mathbf{W}(t)$$

with the initial condition $\mathbf{X}(0) = \mathbf{X}_0$ and $\mathbf{W}(t) = (W_1(t), W_2(t))^t$, where $(W_1(t))_t$ and $(W_2(t))_t$ denote independent Wiener processes. Thus for each population we obtain

$$\begin{aligned}
dc(t) &= \mu_1(c,s)dt + B_{11}(c,s)dW_1(t) + B_{12}(c,s)dW_2(t) \\
&= [a_2(c(t)) + 2a_3(c(t)))b_s s(t) - (a_1(c(t))b_s + d_s)d_c c(t)s(t) - d_c c(t)]dt + \frac{1}{\eta}(u+\tau)dW_1(t) + \frac{v}{\eta}dW_2(t) \\
ds(t) &= \mu_2(c,s)dt + B_{21}(c,s)dW_1(t) + B_{22}(c,s)dW_2(t) \\
&= [a_1(c(t)) - a_3(c(t)))b_s s(t) + (a_1(c(t))b_s - d_s)d_c c(t)s(t) - d_s s(t)]dt + \frac{v}{\eta}dW_1(t) + \frac{1}{\eta}(w+\tau)dW_2(t).
\end{aligned} \tag{1}$$

Thereby, $(c(t))_t$ and $(s(t))_t$ are stochastic processes for which every trajectory describes the evolution of a specific tumor, hence the disease development in a specific patient - if we assume each patient has a single tumor. Thus, $\mathbf{X} = (c,s)^t : \Omega \times (t_0, T) \to (0,\infty)^2$, with $(\Omega, \mathcal{A}, \mathbb{P})$ being a filtered probability space for which Ω denotes the sample space, i.e. a set of tumors/cancer patients.

Remark 2.1 The well-posedness of (1) supplemented with initial conditions

$$c(0) = c_0, \qquad s(0) = s_0 \tag{2}$$

with c_0 and s_0 positive, nonanticipative random variables is not obvious, as the drift and diffusion coefficients are only locally Lipschitz. We refer to [61] for an existence result in the case where $\boldsymbol{\mu}$ and $\mathbb{B}$ are only continuous. The uniqueness needs to be treated separately and there are several works handling this issue, thereby using various notions of uniqueness. When the drift and diffusion coefficients are, however, locally Lipschitz, then strong uniqueness follows, see e.g. [35].
The non-negativity of solutions to our SDE system follows directly from a result by Cresson et al. [10] providing necessary and sufficient conditions for the invariance of rectangular subsets, which we recall for convenience in Subsection 9.1.

2.2 Numerical simulations

In order to simulate our system of SDEs (1) we consider the example of glioma, which are rarely curable brain tumors arising from abnormal glial cells in the human brain, with poor prognosis (the median survival time is about 14 months). We take the birth rate of untreated tumor stem cells to be only very slightly less than the corresponding median value obtained in [62] for glioma, namely $b_s = \log 2/55$. In that paper only one glioma phenotype was observed, thus not distinguishing between stem cells and differentiated cells. As we assumed above that $b_c = 0$, this seems to be justified. For the DCs we assume that their death rate is smaller than the mitosis rate of stem cells, and take $d_c = \log 2/60$. The death rate d_s of CSCs is taken very small, in accordance with the assumptions in Section 2.1. The different rates involved in the probabilities of the CSCs to differentiate are $\widetilde{a_1}$ for the symmetric division into two CSCs, $\widetilde{a_2}$ for the asymmetric division into one DC and one CSC, and $\widetilde{a_3}$ for the division into two DCs. Compared to the symmetric divisions of cancer stem cells, the asymmetric one is much rarer, and is occasionally even neglected (see [26]). We will not completely neglect it, since in our model this would mean that once the DCs get extinct there is no chance of producing any new DCs from the CSCs, which would contradict the biologically well-established fact that tumor relapse can occur from small amounts of stem cells [33]. The parameters used to simulate (1) are collected in Table 2.

Parameter	b_s	d_c	d_s	$\widetilde{a_1}$	$\widetilde{a_2}$	$\widetilde{a_3}$
Value	$\log 2/55$	$\log 2/60$	$\log 2/200$	0.5	0.05	0.1

Table 2: Summary of the model parameters for cancer cells based on [62].

Some trajectories of our SDE system solved with the Euler-Maruyama method and the average over 10^3 such trajectories are shown in Figure 2.

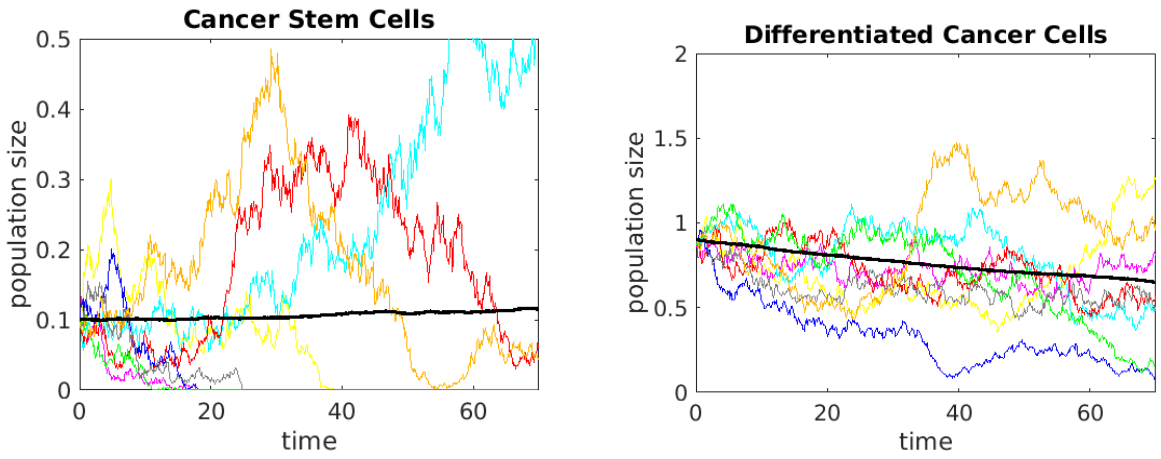

Figure 2: Several trajectories of the solution components of system (1) and averages (black lines) of 10^3 trajectories solved with the Euler-Maruyama algorithm and using parameter values as in Table 2. Initial condition: $(c, s)^t = (0.9, 0.1)^t$.

2.2.1 Approximation of the persistence time

An important aspect of two interacting populations is their long-term behavior, especially the persistence time, i.e. the time it takes for one of the two populations to become extinct. As we consider a system of SDEs it makes sense to look at the mean persistence time of the joint populations. To compute it, we simulate the behavior of the two tumor cell phenotypes described with the aid of the SDE (1) and trace the trajectories until the whole population first becomes extinct. This simulation has to be carried out several times so that we can average the persistence times.
Concretely this means that we generate a large enough number of trajectories (here 1000) by solving (1) with the Euler-Maruyama method over a time span of 70 days. These trajectories are stopped whenever we have $c+s \leq 0$ and we note the exact time of this event. Averaging the data computed with the choice of parameters from Table 2 we obtain estimations for several different compositions of the initial tumor[3], which we collected in Table 3.
Obviously, the computed persistence times are larger when starting with larger tumor cell populations. Just by computing the persistence times is, however, difficult to say whether the tumor heterogeneity plays a role, since these times are only very slightly different when starting with the same overall joint amount of neoplastic cells (compare 3rd to 11th rows in Table 3). They seem to correlate directly with the initial CSC density and inversely with the initial amount of differentiated cells, but there seems to be a balance between these values and the total initial amount is, of course, essential. Biological evidence as reviewed in Section 1 tells, however, that targeting the CSCs should enhance the therapeutic outcome, which is also is suggested by the very simple deterministic model in [13]. We also want to investigate this issue in our stochastic framework. To this aim we study therapy approaches which only use a differentiation promoter and compare them with those also aiming at cell killing by radiotherapy.

[3]by this we mean amount of CSCs and DCs at the initial time, i.e. at the first tumor assessment time; this could be the time of first diagnosis. We do not mean the time at which the tumor started to develop, as that cannot be inferred, and even less its proportions of CSCs and DCs

Initial values $(c_0, s_0)^t$	**Persistence time** (in days)
$(0.01, 0.01)$	16.313
$(0.1, 0.1)$	56.052
$(0.99, 0.01)$	69.463
$(0.8, 0.2)$	69.790
$(0.95, 0.05)$	69.791
$(0.7, 0.3)$	69.799
$(0.4, 0.6)$	69.804
$(0.3, 0.7)$	69.807
$(0.6, 0.4)$	69.871
$(0.9, 0.1)$	69.892
$(0.5, 0.5)$	69.909
$(1, 1)$	70

Table 3: Persistence times for the whole tumor $c + s$, averaged over 1000 trajectories, for different compositions (c, s) of the initial tumor.

3 Including treatment

Cancer stem cells have been identified in many tumors as the driving force behind cancer growth as well as cancer progression [26]. Consequently, effective treatment schedules and strategies should affect the differentiated cancer cells as well as the cancer stem cells. The eradication of CSCs is rather difficult, as these cells are less sensitive to radiation or chemical agents in comparison to DCs [50]. Moreover, it is difficult to identify these cells in vivo, as they are spread all over the tumor [68].
An important consequence of cancer treatment is the increase of the death rates d_c and d_s for both types of cancer cells. In this section we present and illustrate the main therapy concepts by showing their respective effects on the tumor cells only. Their application to the tumor and normal cells will be addressed in Section 5.

3.1 Chemotherapy: differentiation promoters

In chemotherapy different cytotoxic agents affect the death rate of the DCs as well as that of CSCs, depending on the treatment dose. CSCs are less sensitive to this treatment, resulting in a lower death rate in comparison to the DCs [50].
Here we present an approach to model the so-called differentiation therapy. Here the aim is to induce the cancer cells to resume the process of maturation. This kind of therapy does not directly kill the cancer cells, but restrains their growth and allows the more efficient application of conventional therapies to eradicate the tumor. Thereby, the sensitivity of cancer stem cells is enhanced by adding differentiation promoting agents. Possible promoters are members of the TGF-β superfamily which are known to affect the characteristics of growing tumors like invasion and immune evasion, and most important (as mentioned), the increase of stem cell differentiation [26].
In our model from Section 2.1 this would imply decreasing the probability a_1 which characterizes the splitting of a cancer stem cell into two cancer stem cells, and increase the probability a_3 for the differentiation of a cancer stem cell into two differentiated cancer cells. Here we focus on the fact that the rate a_3 depends on the parameter δ related to the dose of the chemical differentiation promoter delivered during the treatment. Thus, we get

$$a_3 = a_3(c, \delta) = \frac{\tilde{a}_3(\delta)c}{\tilde{a}_1 + \tilde{a}_2 c + \tilde{a}_3(\delta)c}, \quad \text{with } \tilde{a}_3(\delta) = \tilde{a}_3 + \frac{\tilde{\alpha}\delta}{1+\delta}, \qquad \tilde{\alpha} > 0, \tag{3}$$

where $\tilde{a}_3$ is the value in the case without therapy and $\tilde{\alpha}$ is a sensitivity parameter. For instance, drugs targeting histone deacetylases (HDACS) are already being used to enhance differentiation or reprogramming events; we refer to [46] for a review of epigenetic alteration agents involved in CSC reprogramming. A treatment approach in a phase I study is to deliver 200 mg bid per day of SAHA (vorinostat) on 7 days a week, with one treatment cycle of 4 weeks [36]. Low grade gliomas have diameters between 1 and 6 cm (occasionally even larger), see e.g., [7]. We choose an early stage tumor with a diameter between 1

and 2 cm, hence a reasonable dose in a tumor of diameter 1.2 cm can be assumed to be $\delta = 0.05625$ mg.[4] In addition to a change in differentiation rates, the chemotherapy also influences the cell death rate depending on the dose. We assume an increase in the death rate for the differentiated cancer cells with 0.015, which is comparable to the one in [53]. Due to the fact that cancer stem cells are less sensitive to this supplementary therapy effect we only increase the death rate with $d_s = 10^{-4}$.

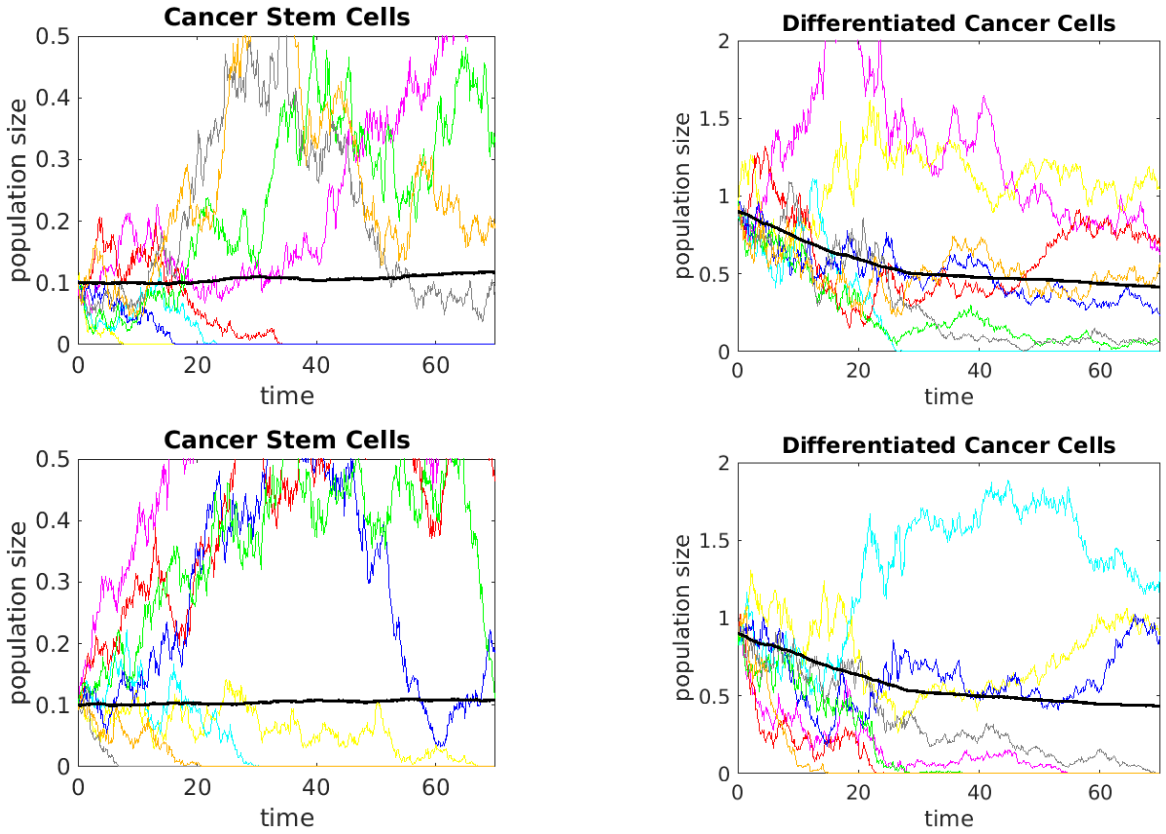

Figure 3: Different trajectories of the SDE system (1) and their averages (thick black lines) for 10^3 trajectories when applying chemotherapy. Parameter values as in Table 2, dose-dependent probability a_3 of symmetric splitting of a cancer stem cell into differentiated cells as given in (3). Upper row: $\tilde{\alpha} = 0.5$, lower row: $\tilde{\alpha} = 10$.

Trajectories obtained by numerical simulations with the Euler-Maruyama method for widely different values of the sensitivity parameter $\tilde{\alpha}$ are shown in Figure 3. The sensitization on CSCs effects a slightly reduced growth in their density, while the DCs are depleted to a certain, however not very large amount. For (much) larger values of $\tilde{\alpha}$ there is even less increase in CSCs (but no effective decrease) and almost no further effect on DCs, but the concrete choice of this parameter seems to be hardly of relevance with respect to the efficacy of reducing the overall tumor burden when the effect of the chemotherapeutic agent is mainly aiming at sensitizing the cancer cells by inducing differentiation of CSCs. The behavior of CSCs and DCs is shown including the follow-up time of 42 days after the end of this treatment. The depletion is too low (compare also with Figure 2 showing no therapy at all), as the cancer stem cells are known to trigger recidives even when present in a very low amount [33]. Therefore this approach alone is not enough to control the tumor: The differentiation promoter should be used in an adjuvant way with other therapies, e.g. ionizing radiation.

3.2 Radiation therapy

When applying radiotherapy proliferating cells are harmed by altering their genetic material. Depending on the cell type and the cell's current position in the cell cycle, its radiosensitivity varies.
The most common approach for modeling the radiation treatment of a tumor is the LQ-model based on

[4] for simplicity we assume this to be constant

a linear-quadratic exponent to describe the effect of the therapeutic dose on cell survival fractions: A cell survives applied doses of radiation (and is said to be a clonogen) if it is able to act as a progenitor for a significant line of offspring [11]. The fraction of surviving cells $S(D)$ after a single total dose D (in Gray) is then given by (see e.g., [4])

$$S(D) = e^{-(\alpha D + \beta D^2)} \tag{4}$$

for parameters α, β that correlate with the cell cycle length. The parameter α can be interpreted as the lethal damage due to a single track of radiation and the parameter β represents lethal damage due to the misrepair of DNA damage as a result of two separate tracks of radiation [26]. Tissues with a slow cell cycle correspond to a small α/β-ratio, whereas fast cycling tissues containing quickly proliferating cells correspond to a larger α/β-ratio. In common clinical practice the total dose D is given in ν fractions of equal size d [4]. From the corresponding hazard rates

$$d_i = (\alpha_i + \beta_i d)d \qquad \text{for } i = c, s \tag{5}$$

we obtain the death rates involved in system (1). Unlike chemotherapy in the previous section, the treatment with radiation includes weekend breaks. A common daily radiation dose is $d = 2$ Gy during $\nu = 25$ days of treatment (hence a total dose of 50 Gy, leading to an overall treatment time of 5 weeks [4]. To simulate this therapy strategy we choose the sensitivity parameters in Table 4. The obtained results are shown in Figure 4.

Parameter	α (in Gy^{-1})	β_c (in Gy^{-2})	β_s (in Gy^{-2})	d (in Gy)	ν (in days)
Value	0.0906	0.006	0.00605	2	25

Table 4: Model parameters for radiation therapy based on [54, 67], where no difference was made between various phenotypes of tumor cells. The parameter β_s was chosen here slightly larger than β_c to account for the reduced sensitivity of CSCs towards therapy.

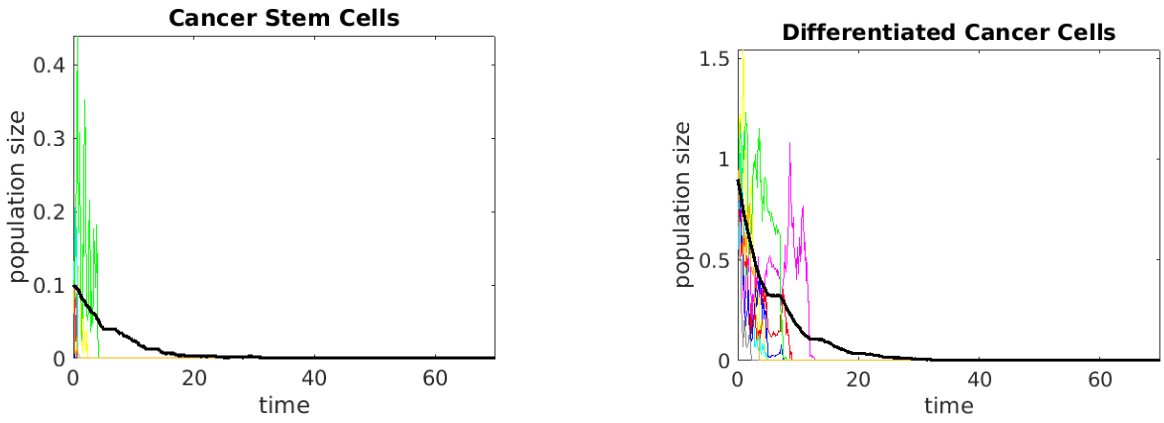

Figure 4: Different trajectories of the solutions components of system (1) with the application of radiation therapy and their averages (thick black lines) over 10^3 trajectories. Parameter values as in Tables 4 and 2, follow up to 70 days.

A closely related concept to the LQ-model is the Biological Effective Dose (BED) [4]. This quality measure of radiation treatment only involves the exponent of the LQ-model and has the form

$$\text{BED} = \nu d\Big(1 + \frac{d}{\alpha/\beta}\Big) \tag{6}$$

with the dose d per fraction and the number of fractions ν. We will use this quantity in Subsection 3.4 to describe therapy applying irradiation doses at discrete times, alone or in combination with the continuous application of a cell differentiation promoter.

3.3 Combining chemotherapy and radiotherapy

Most patients undergo tumor resection for diagnostic and treatment purpose, however postoperative treatment strategies like radiation and chemotherapy are needed to further reduce tumor progression and

ideally prevent recurrence. Thereby, they can be used in a consecutive or concurrent way; the latter option seems to be often the better choice [6, 20]. Clinical trials aiming at the investigation of such combined effects have been set up; for instance, the use of vorinostat together with radio and chemotherapy (cisplatin) in the treatment of advanced staged oropharyngeal squamous cell carcinoma makes the object of a phase I study (ClinicalTrials.gov identifier NCT01064921). Studies of histone deacetylase inhibitors as anticancer drugs in combination with radiotherapy have been performed for a large variety of cancers, including glioblastoma, see [15] and references therein.

In our model we consider the joint application of a differentiation promoter (e.g., vorinostat) and of radiotherapy. As mentioned above, the main effect of chemotherapy is the stimulation of differentiation into cells which are more sensitive towards radiotherapy, thus boosting the cell kill. However, the administered drug can also induce a modest cell depletion by itself, hence enabling us to add some tiny, but positive constants to the previous death rates d_s and d_c used in our model obtained in Section 2. For simplicity we consider a simulation based approach and do not incorporate a decay term modeling radiation therapy via the LQ model into our system of SDEs, but simply apply formula (4) to the CSC and DC volume fractions at scheduled times during computation. The simulation is stopped at the times of radiation treatment, $S(D)$ is applied to c and s using the corresponding values for α and β, and then the simulation is resumed. The radiotherapy is applied 5 days a week, 5 weeks, with a daily dose of 2 Gy, resulting in a total therapy time of 35 days. Chemotherapy (sensitization) follows the approach in Subsection 3.1 above and involves the same dose therein, applied daily in a concurrent way during the time span of 4 weeks and during all weekdays. The administration of the chemotherapeutic agent leads to an increase in the number of CSCs dividing symmetrically into DCs and thus becoming more sensitive to radiation. Simulations of this combined treatment strategy are shown below in Figure 5. Just by visually comparing this with Figure 4 it is difficult to decide whether radiotherapy gives better results alone or in simultaneous combination with a differentiation promoter.

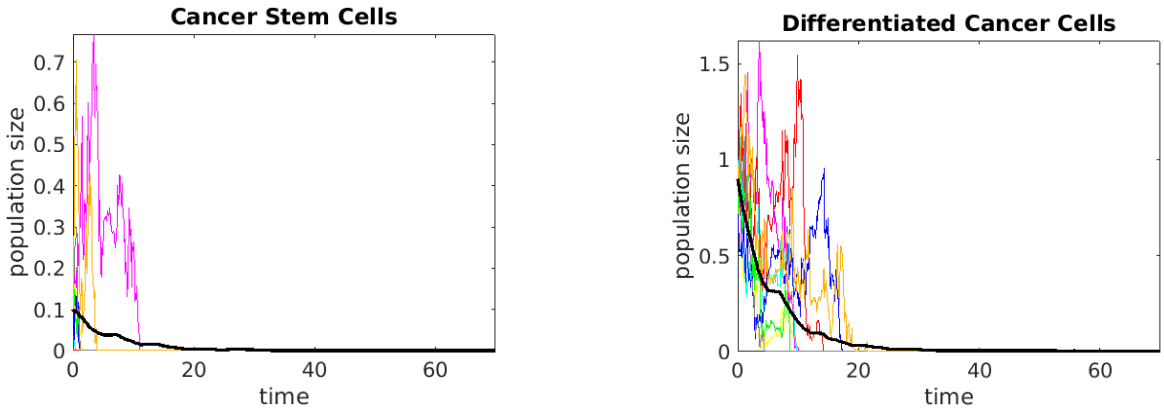

(a) (b)

Figure 5: Trajectories of the SDE model (1) with the simultaneous application of radio- and chemotherapy (differentiation promoter) and their averages (thick black lines) over 10^3 simulated trajectories. Parameter values as in Tables 4 and 2, with $\tilde{\alpha} = 10$, follow up to 70 days.

A further common way to integrate different cancer therapies is to alternately apply chemotherapy (in our case differentiation promoter of CSCs into DCs) and ionizing radiation. Thereby, an often used schedule is to apply three to four weeks of chemotherapy followed by radiotherapy. Here a differentiation promoter is administered for 4 weeks and subsequently radiotherapy is applied for 5 weeks, only on workdays, to achieve a total dose of 50 Gy in fractions of 2 Gy each. The parameters are chosen in accordance with the previous Subsections 3.1 and 3.2. The results of the corresponding simulations are depicted in Figure 6.

Upon comparing the two approaches involving combined chemo- and radiotherapy we observe that the consecutive application seems to be less efficient than the concurrent one.

3.4 Time-discrete therapy

Up to now we have considered the development of the population sizes of cancer stem cells and differentiated cancer cells for continuous therapies. However, no treatment schedule is actually continuous,

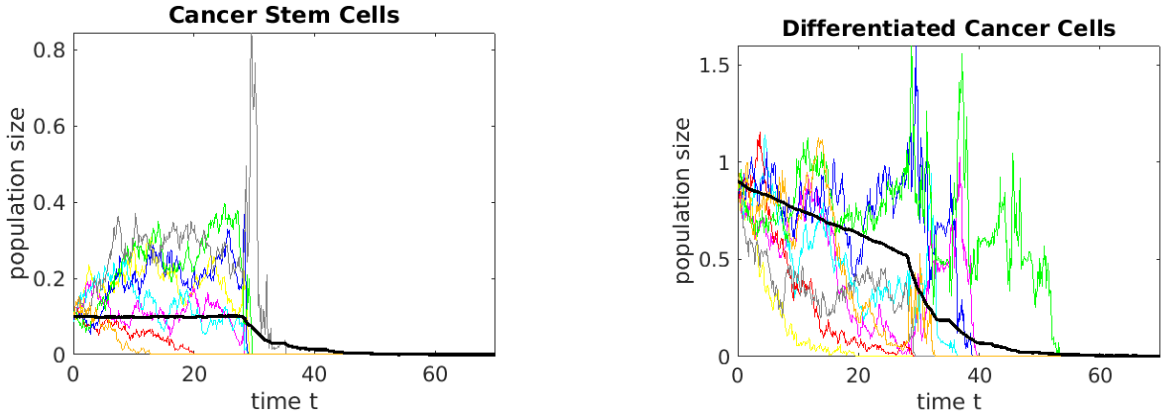

(a) (b)

Figure 6: Different trajectories of the SDE model (1) with the alternating application of chemotherapy and radiation therapy and their mean values (thick black lines) for 10^3 simulated trajectories. Parameter values as in Tables 4 and 2, with $\tilde{\alpha} = 10$, follow up to 70 days.

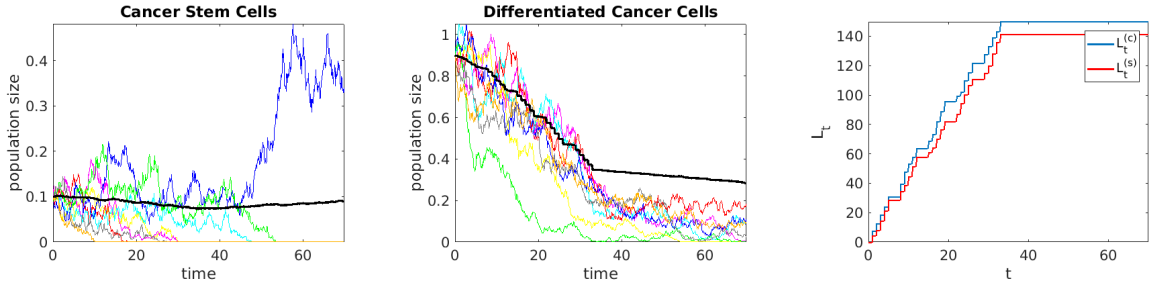

(a) (b) (c)

Figure 7: Trajectories of (1) and their averages (thick black lines) over 10^3 simulated trajectories with a time-discrete radiotherapy solved with the Euler-Maruyama scheme, parameter values as in Table 2. Subfigures 7(a) and 7(b) show the results of the simulation for the two subpopulations of cancer cells and 7(c) shows the processes $L_t^{(s)}$, $L_t^{(c)}$.

therefore we model a time-discrete approach involving chemo and/or radiation therapy, in a way that it is typically applied to patients, i.e. at discrete points in time - for example: once a day, except for weekends.
To this aim we select a sequence of points in time $\{t_k\}_{k=1,\dots,N}$ with $0 < t_1 < \dots < t_N$ at which the treatment is administered. Further let $\xi_1, \dots, \xi_N$ be a sequence of i.i.d. random variables characterizing the effect of therapy on the tumor cells. Thus, the random variable ξ_k corresponds to the treatment at time t_k. The process L_t describes the (cumulative) effect of the treatment on the respective cell types and can be given e.g., as in [65]

$$L_t^{(j)} = \begin{cases} 0 & , \text{if } 0 \le t < t_1 \\ \sum_{\{k:\ t_k \le t\}} \xi_k^{(j)} & , \text{if } t_1 \le t. \end{cases} \qquad j = c, s. \tag{7}$$

Thereby we set $\xi_k^{(j)}$ to be a rescaled non-centered χ^2-distributed random variable

$$\xi_k^{(j)} \sim \sigma_D \chi^2 \left(1, \mathrm{BED}^{(j)}\right) \tag{8}$$

with $\mathrm{BED}^{(j)}$ representing the biological effective dose from (6) computed for α_j/β_j, the parameter values $\sigma_D = 0.1$, $d = 2$ Gy, and the corresponding sensitivity parameters α_j, β_j $(j = c, s)$ as in Table 4.
Next we need a couple of stochastic processes $R_c(t)$ and $R_s(t)$ that characterize the population sizes of the differentiated cancer cells and the cancer stem cells upon application of therapy:

$$R_c(t) = c(t) e^{-\varepsilon_c L_t^{(c)}}, \qquad R_s(t) = s(t) e^{-\varepsilon_s L_t^{(s)}} \tag{9}$$

for $t \geq 0$ with small constants $\varepsilon_c, \varepsilon_s > 0$ (here we choose $\varepsilon_c = 0.0004$, $\varepsilon_s = 0.0002$ to account for the stem cells being less sensitive). The choice of the noncentral parameter of the χ^2 distribution is motivated by the proportionality between the mean of ξ_k and the dose d; this dependence is analogous to that for the survival fraction, hence (9) actually describes the effect of radiotherapy (LQ model) on the respective population of tumor cells. In order to simulate this model we need some distributions and parameters that we choose similarly to Section 2.2, Table 2. When applying radiotherapy alone or simultaneously to the continuously applied differentiation promoter we start the radiation treatment at time $t_1 = 1$ and continue on every workday, for 5 weeks, if applicable administering during the weekends the chemotherapeutic agent for cancer cell sensitization. Simulations of the application of radiotherapy alone are depicted in Figure 7. In this case, too, after the end of treatment the cancer cells (especially CSCs) multiply further and trigger recurrence of the tumor, so that applying a differentiation promoter is expected to lead to a better outcome.

The application of radiotherapy at discrete times can also be combined in an alternative way with the continuous administration of differentiation promoter (i.e. first chemotherapeutic sensitization by differentiation promoter for 4 full weeks, then radiotherapy applied once a day during the 5 weeks following chemo, only on workdays). In the next section we will assess the effects of these and the previous approaches by way of TCP.

4 Treatment assessment via TCP

A common quality measure for the success of a treatment schedule is the tumor control probability (TCP), which gives the probability that no clonogenic cell survive radiation treatment. It is determined by complex interactions between tumor biology, tumor microenvironment, radiation dosimetry, and patient-related variables. The complexity of these joint factors constitutes a challenge for building predictive models for routine clinical practice.

Most TCP models rely on simple statistics connected to cell survival. Among these, the model considering a discrete distribution (Poisson or binomial) for the number of cells surviving radiation treatment is –due to its simpliciy– very popular, see e.g., [8]. These settings, however, cannot capture many of the features related to the specific treatment schedules, like cell repair, proliferation, sensitivity to radiation etc. Cell population models describing the evolution of the tumor cell density via differential equations offer a way to overcome these drawbacks, but most of those considered so far are purely deterministic, hence adequate only for large cell populations. By anti-cancer therapy, however, such a population is supposed to shrink drastically, so that only a small number of cells remains. As already mentioned in Section 1, this renders the use of a deterministic model questionable, thus calling for the accommodation of stochasticity in the modeling process. Settings accounting for uncertainties via stochastic birth and death processes have been proposed e.g., by Zaider and Minerbo [69] and extended e.g. in [11, 22]; they lead eventually to a system of ODEs, which are the mean field equations for the expected cell density -thus carrying, in fact, the assumption of large cell populations- and where the effect of the birth and death processes is captured via a hazard function. Here we assess the TCP from our SDE models introduced above, thereby relying for its computation on numerical simulations, as a closed form expression of the TCP (as obtained e.g., in [11, 22]) seems to be out of reach, given the complexity of such formulations. We denote by τ_{c+s} the first time when the stochastic process characterizing the overall tumor cell population first becomes zero and compute (following the idea in [65])

$$\mathrm{TCP}(t) = \mathbb{P}(\tau_{c+s} \leq t), \qquad t \geq 0. \tag{10}$$

This implies that the TCP is the cumulative distribution function of the random variable τ_{c+s}. Based on (10) we can thus compute the TCP upon performing a large number Q of simulations for the process $(c+s)(t)$:

$$\mathrm{TCP}(t) = \frac{\text{number of simulations with } \tau_{c+s} \leq t}{Q}, \tag{11}$$

which is a probability that converges to $\mathrm{TCP}(t)$ for $Q \to \infty$. The results are shown in Figure 8. The comparison between TCPs for the different therapy approaches gives some hints on which of these might be more effective with respect to tumor eradication.

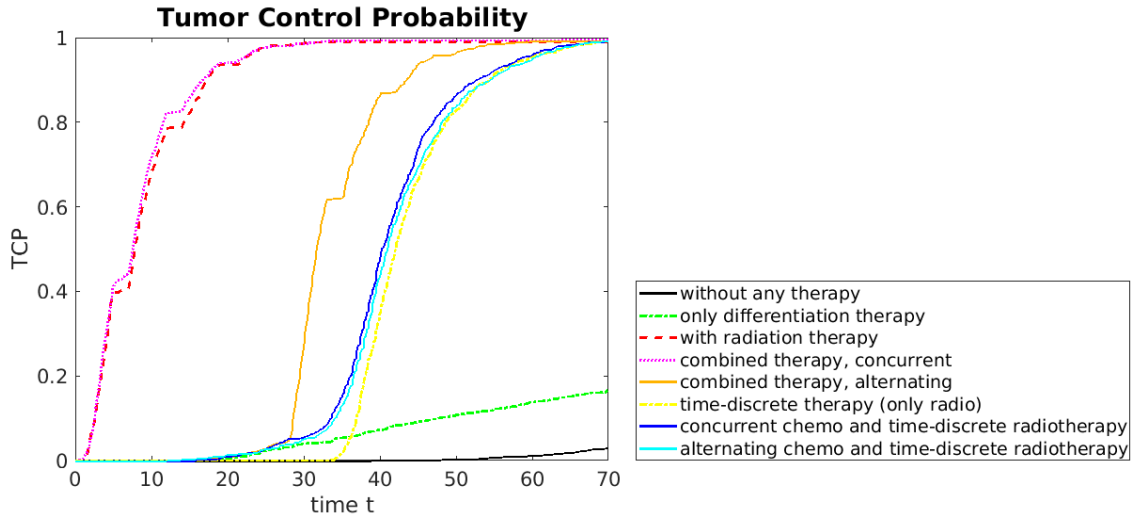

(a)

Figure 8: TCP for the different therapy strategies based on (1), with 10^3 simulations.

However, the treatment should not have the single aim of eradicating the neoplastic tissue; preserving as much healthy tissue as possible is of utmost importance as well. Therefore, the effects of therapy on the normal tissue have to be included in the models. They are influenced, too, by the stochasticity inherent to the system and are addressed in the next section.

5 SDE formulation accounting for the effects on normal tissue

Analogously to Section 2.1 we can derive an SDE for the normal cell density:

$$dn(t) = (b_n - d_n)n(t)dt + \sqrt{(b_n + d_n)n(t)}dW(t) \tag{12}$$

with initial conditions $n(0) = n_0$ and the Wiener process $W(t)$ assumed to be independent of $W_1(t)$ and $W_2(t)$ in (1). The dynamic death rate d_n is defined as

$$d_n(t) = h_n(t) + \delta_n(t)(S_c(D)c(t) + S_s(D)s(t)), \tag{13}$$

where $\delta_n(t)$ characterizes the interaction between normal tissue and tumor cells, which is known to be destructive for the former, due e.g. to tumor-induced hypoxia and the effects of matrix degrading enzymes. However, only living tumor cells can degrade the normal tissue, therefore we have to include the survival fractions for both cancer cell phenotypes, according to their sensitivities toward the applied treatment. When no radiotherapy is applied we take $S_c = S_s = 1$. We further assume that in the time span of interest the natural decay of normal tissue (i.e. without any influence of therapy or cancer) is negligible. The term $h_n(t)$ describes normal tissue necrosis due to therapy; concretely, $h_n(t)$ denotes the hazard rate of normal cells and can be seen as an intrinsic risk of being degraded by therapy. A classical choice is $h_n(t) = -(\ln(S(t)))'$, where $S(t)$ represents the dynamic survival fraction of normal cells under therapy, see e.g., [59]. When considering therapy according to the LQ model this leads to

$$h_n(t) = (\alpha_n + 2\beta_n D(t))\dot{D}(t),$$

with the positive constants α_n and β_n denoting as before the sensitivity parameters and $D(t)$ being the total dose absorbed at time t. Analogous formulae hold for the other cell subpopulations (CSCs and DCs) as well (with corresponding sensitivities α_i and β_i, $i = c, s$). When the total dose is fractionated, i.e. $D = \nu d$, then in [23] the hazard rate was proposed to take the form

$$h_n(t) = (\alpha_n + \beta_n d)\dot{D}(t). \tag{14}$$

Furthermore, considering as in [22] t_i $(i = 1, \ldots, \nu)$ the starting time of each fraction and assuming the doses are delivered during the time interval $[t_i, t_i + R_T]$ with a constant amount d in each fraction (R_T denotes thereby the fraction length, here $R_T = 1$), following [22] we arrive at

$$\dot{D}(t) = \begin{cases} d, & t \in [t_i, t_i + 1] \\ 0, & \text{otherwise} \end{cases},$$

which makes of (14)

$$h_n = (\alpha_n + \beta_n d)d.$$

The survival fractions are modified correspondingly to account for this fractionation, so that for each treatment fraction we use $S_c(d)$ and $S_s(d)$ in (13). With this the death rate in (13) is completely specified and we turn our attention toward the birth rate b_n in (12). Aligning to a logistic growth model (see also [22, 64]), we assume this birth rate to depend on an organ specific carrying capacity M and take

$$b_n(t) = \begin{cases} \mu_n \left(1 - \frac{n(t)}{M}\right), & \text{if } n(t) \leq M \\ 0, & \text{otherwise} \end{cases}, \tag{15}$$

to be the birth rate if $n(t)$ normal cells are alive. This implies that the normal cell growth is limited by growth factors like space and nutrient supply. Due to this definition an increasing population size leads to a decreasing birth rate. With this choice the amount of normal cells would always stay below the carrying capacity M if we would only examine the deterministic model. Setting $b_n(t) = 0$ whenever n exceeds the carrying capacity (which can happen when describing stochasticity upon using a Wiener process) a too large increase of the normal tissue is prevented.
Observe that the dynamics of normal cells is (unidirectionally) coupled to that of CSCs and DCs via decay induced by the interaction between healthy and neoplastic tissues. Thus, in order to assess the evolution of $n(t)$ we need to solve the SDEs for $c(t)$ and $s(t)$ introduced and handled in Sections 2 and 3. Numerical simulations of solutions to (12) with the coefficients described above are shown in Figure 9 for the case with no therapy. Thereby we introduce a threshold density for the normal tissue: If the latter falls below that threshold, then the respective area affected by the tumor is assumed to no longer function. From this point on we will fix this threshold to $\gamma = 0.7$, meaning that the affected region will collapse when less than 70% of its constituent tissue is functional. Notice that without therapy (i.e. for $h_n(t) = 0$ and $S_s = S_c = 1$ in (13)) the (average) normal tissue density will reach the threshold γ in more than the observed 70 days. The next step will be to take treatment into account.

Parameter	Description	Value
μ_n	constant maximum birth rate (in day^{-1})	0.01
δ_n	interaction factor	0.002
γ	threshold of functionality	0.7
n_0	initial density of normal tissue	1
M	actual carrying capacity (normalized)	1

Table 5: Model parameters for normal tissue (without therapy).

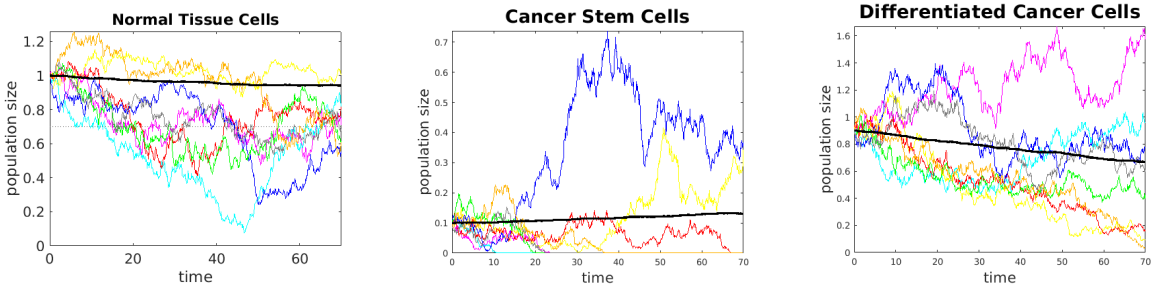

Figure 9: Trajectories of (12) for normal tissue density and of CSCs and DCs as solutions to (1). Their averages over 10^3 trajectories are shown as thick black lines. Parameter values are given in Table 5. The dotted grey line represents the threshold value γ for the normal cell density.

The application of chemotherapy (only aiming at CSC differentiation into DCs) does not explicitly alter the equation in our model (12). However, it affects indirectly the normal tissue density, on the one hand by reducing the amount of tumor cells and thus decreasing the normal tissue degradation, but on the other hand due to the side effects of the differentiation promoter it can also degrade a certain (very small) amount of tissue. Simulations of the behavior of normal cells with a differentiation promoter therapy as

described in Section 3.1 are shown in Figure 10. Only very small differences between the situation with no therapy and that with application of the differentiation promoter can be observed; the cancer cell densities seem to be slightly reduced when therapy is applied, while the normal cells are hardly affected. In average the normal tissue maintains its function beyond the time span of the treatment schedule (4 weeks).

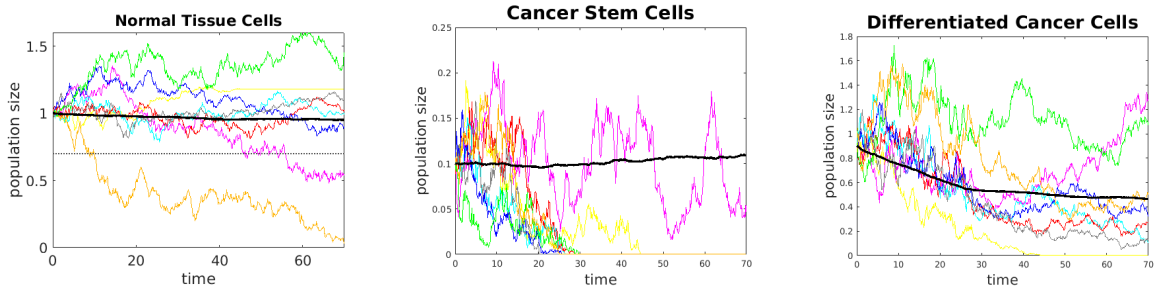

Figure 10: Trajectories of (12) for normal tissue density and of CSCs and DCs as solutions to (1) for the differentiation therapy approach in Section 3.1, with $\widetilde{\alpha} = 10$. Their averages over 10^3 trajectories are shown as thick black lines. Parameter values are given in Table 5. The dotted grey line represents the threshold value γ for the normal cell density.

Now including radiotherapy (i.e. taking a nonzero hazard rate $h_n(t)$) increases the death rate of normal tissue. We consider as before several treatment approaches, including radiotherapy alone or in combination with the differentiation promoter, in concurrent or alternating ways. Time-discrete scenarios are also considered: Figure 11 shows simulations of the densities of normal cells, cancer stem cells, and differentiated cancer cells for these approaches. In the time-discrete case we illustrate in Figure 12 the outcome for radiotherapy applied at discrete times (on 25 days, once a day, during workdays, each dose 2 Gy), alone or in combination with differentiation therapy applied continuously for a period of 4 weeks and for an alternating therapy with differentiation promoter applied continuously for 4 full weeks, followed by time-discrete radiotherapy applied for 5 weeks (working days only, 2 Gy once per day). For the simulations we use the parameters from Tables 5 and 6.

Parameter	Description	Value
α_n	sensitivity parameter (in Gy^{-1})	0.0025
β_n	sensitivity parameter (in Gy^{-2})	0.003

Table 6: Model parameters for radiotherapy affecting normal tissue, based on [22].

6 Treatment assessment: NTCP and UTCP

Normal tissue complication probability (NTCP) and uncomplicated tumor control probability (UTCP) are two further measures for the quality of treatment. They aim at assessing its damaging influence on the normal tissue alone (NTCP) and jointly on tumor cells and normal tissue (UTCP). NTCP is generally defined as the probability that the functioning of normal tissues is impaired by exposure to ionizing radiation and is hence to be kept as low as possible. There are quite a few approaches to computing NTCP for diverse treatment schedules described in a deterministic way or including stochasticity via birth and death processes, see e.g., the Lyman model [43] using dose-volume histograms and applicable to uniform dose distributions, its adaptation to nonuniform distributions done in [41], further extensions like the critical volume NTCP model [32, 48] accounting for the tissue structure, i.e. whether parts of it can still function if the rest is damaged, and the model presented in [22] relying on simple birth and death processes and allowing to compute the NTCP by way of generating functions or numerical simulations. The method applied in [64] to determine a formula for NTCP cannot be used here, as our framework is more complex and does not allow to perform the assumptions made therein. In the following we therefore compute the NTCP with the aid of numerical simulations from our SDE model.

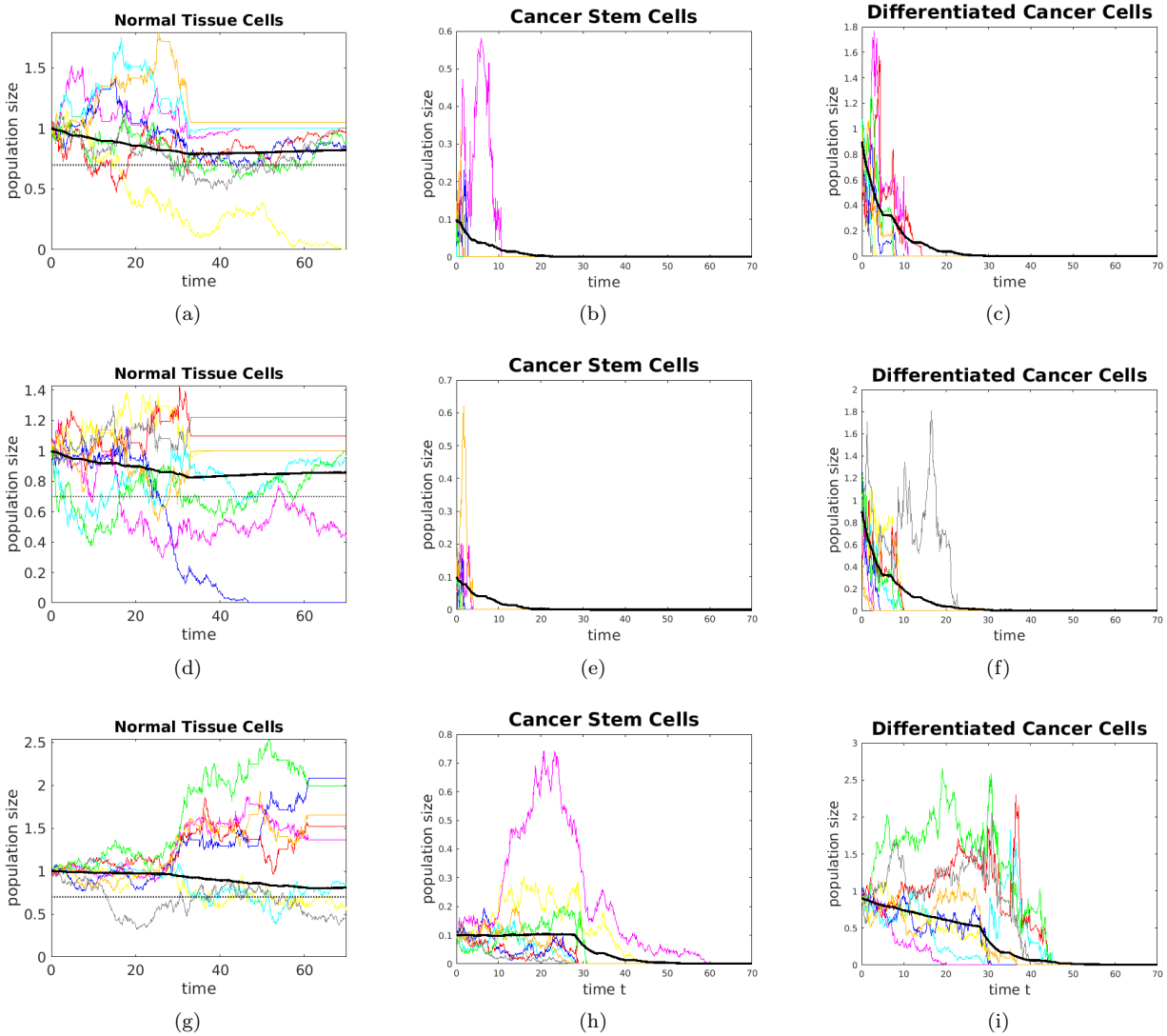

Figure 11: Trajectories of the SDE (12) and of system (1) and their averages (black lines) over 10^3 trajectories. Parameters as in Tables 2, 4, 5 and 6. Plots 11(a)-11(c): effect of radiation therapy only. Plots 11(d)-11(f): concurrent chemo and radiotherapy. Plots 11(g)-11(i): alternating chemo and radiotherapy.

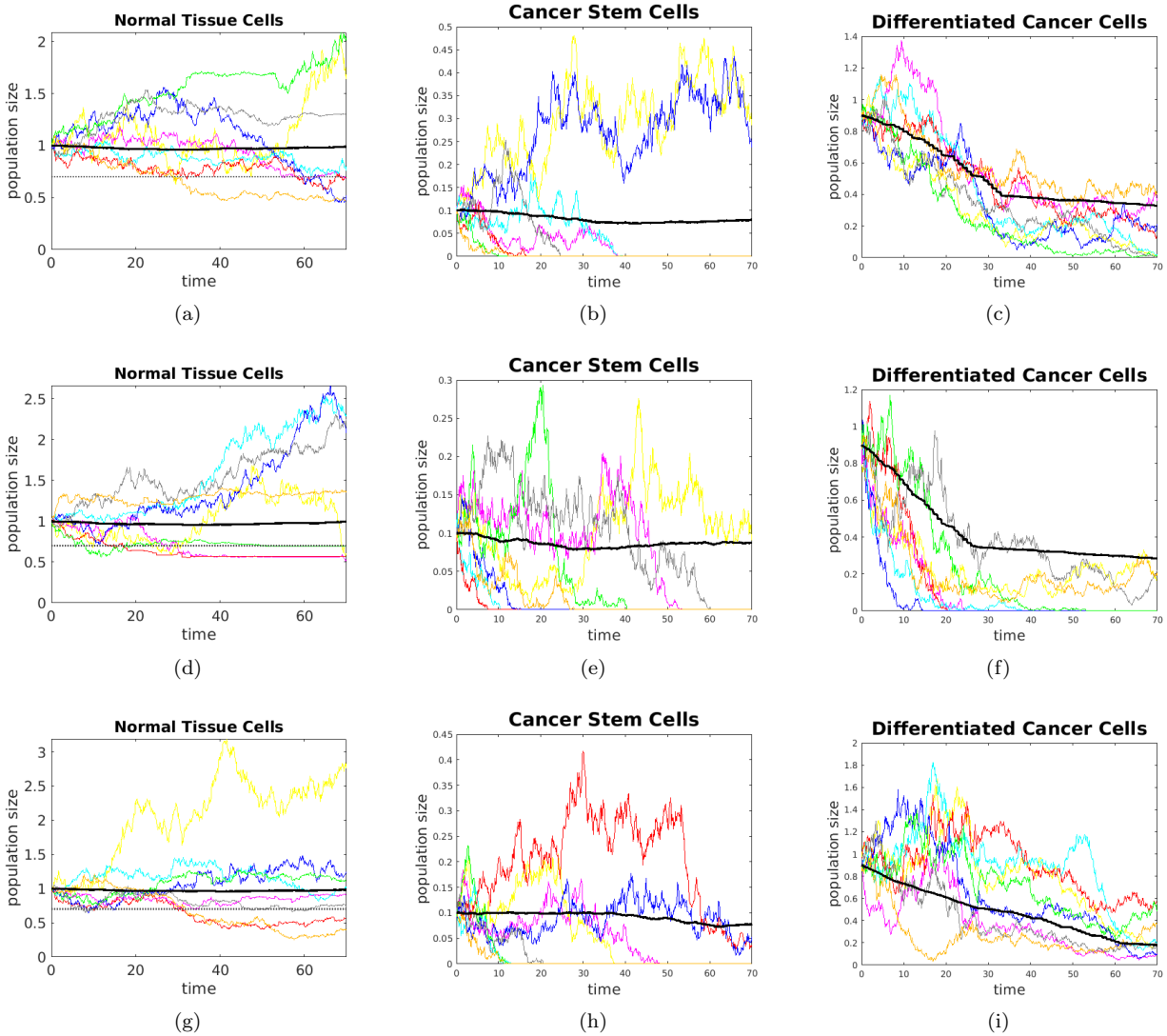

Figure 12: Trajectories of the SDE (12) and of processes $c(t)$, $s(t)$ obtained by applying time discrete therapy: radiotherapy alone (plots 12(a)-12(c)); in a concurrent (plots 12(d)- 12(f)) or an alternating way (plots 12(g)-12(i)). Averages over 10^3 trajectories are shown in thick black lines. Parameters as in Tables 2, 4, 5 and 6.

NTCP computation for an SDE model In analogy to Section 4 we denote by τ_n the random variable registering the times when $n(t)$ first drops below a specific threshold value γ. This threshold γ describes as in Section 5 the minimum amount of normal tissue necessary for a specific organ to function properly. Then the probability that severe complications occur in the healthy tissue is given by:

$$\text{NTCP}(t) = \mathbb{P}(\tau_n \leq t) \qquad t \geq 0. \tag{16}$$

This implies that the NTCP is the cumulative distribution function of the random variable τ_n. As our differential equations are quite complex we cannot explicitly compute a formula for the NTCP but we can approximate it numerically.
Based on (16) we can compute the NTCP upon simulating a large number Q of trajectories for the process $n(t)$ denoting for the volume fraction of healthy tissue and obtain

$$\text{NTCP}(t) = \frac{\text{number of simulations with } \tau_n \leq t}{Q}, \tag{17}$$

which converges to NTCP(t) for $Q \to \infty$. Simulating the NTCP via the SDE model and with parameters given in Tables 5 and 6 we obtain the results presented in Figure 13. As expected, the time-discrete

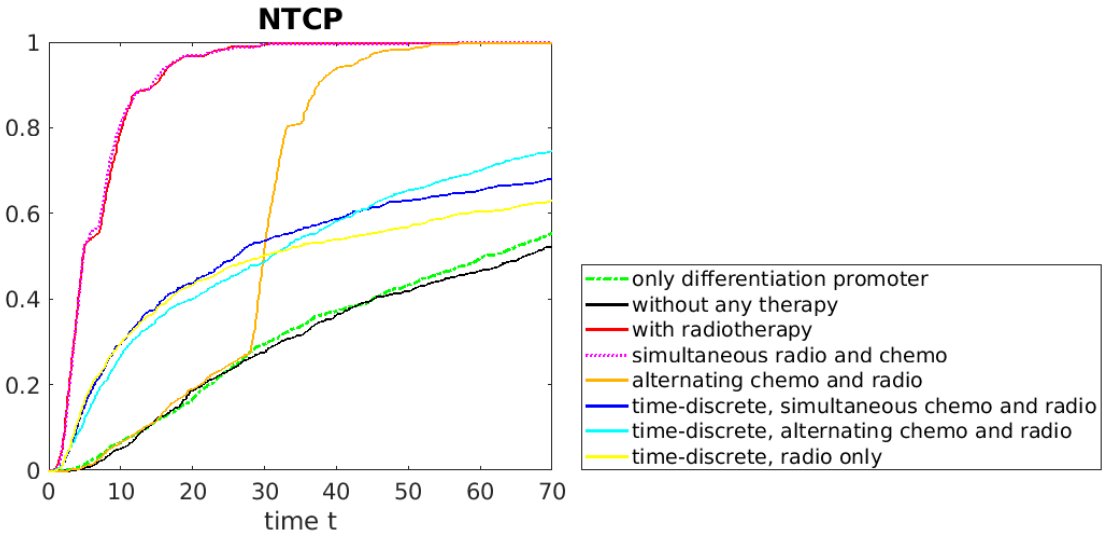

Figure 13: NTCP for the different therapy strategies based on SDEs, 10^3 simulations.

therapy approaches seem to be the more conservative ones. The mere use of a differentiation promoter is the approach least damaging the normal tissue, but it is also least efficient in killing cancer cells, while time-discrete approaches are comparable. A high efficiency in tumor cell depletion is unfortunately impairing the functionality of normal tissue, therefore another quality measure is needed to assess the performance of a therapeutic approach.

Uncomplicated Tumor Control Probability In Sections 4 and 6 we have computed and estimated values for the TCP and NTCP with different models. For an effective treatment we do not only have to increase the TCP but also keep the NTCP at a minimum. Therefore, we introduce the uncomplicated tumor control probability (UTCP) which is a general expression for the probability of achieving complication-free tumor control [34].
In general, the UTCP can be described as the probability for tumor control (denoted with $P(C)$) minus the probability that the patient suffers severe health impairment (denoted with $P(I)$) but is controlled:

$$\text{UTCP} = P(C) - P(C \cap I), \tag{18}$$

where $P(C \cap I)$ denotes the probability that the tumor is controlled and the patient suffers health impairment [1]. With the multiplication law of statistics, we can rewrite (18) as

$$\text{UTCP} = P(C) - P(C)P(I|C) = P(C)(1 - P(I|C)),$$

where $P(I|C)$ is the conditional probability for injury provided the tumor has been controlled. When the event of an injury I and the event of tumor control C are statistically independent we obtain $P(I|C) = P(I)$. Thus we obtain

$$\text{UTCP} = P(C)(1 - P(I))$$

which is

$$\text{UTCP} = \text{TCP}\,(1 - \text{NTCP}) \tag{19}$$

with our notations from the previous sections. Figure 14 shows results obtained by simulating the previous therapy strategies relying on (1) and (12). Averages are taken over 10^3 simulations. The results suggest that time-discrete therapies start becoming a more effective option after the half time of overall treatment, while continuous time approaches seem to be adequate only during the earlier treatment phase, though their UTCPs are quite low. Moreover, the UTCP of radiotherapy alone or applied concurrently with the differentiation promoter seems to perform better than that of alternative chemo-radiotherapy, which suggests that at least in the continuous case the use of a differentiation promoter is questionable. However, as mentioned previously, radiotherapy is actually applied in a time-discrete way. The UTCP obtained in this case also suggests that the application of a differentiation promoter as sole chemotherapy might not lead to substantial benefit (at least when compared with radiotherapy); it is merely the earlier onset of positive therapeutic effects which could justify its use.

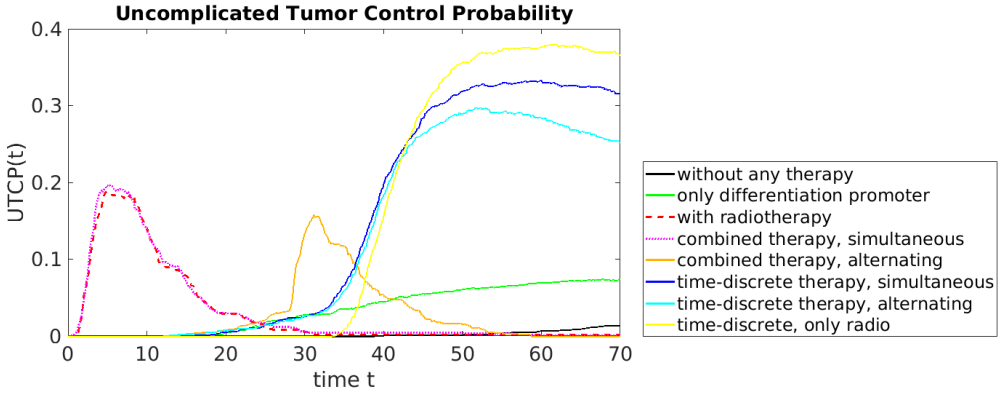

Figure 14: UTCP for the different treatment strategies based on 10^3 simulations of (1) and (12).

Probably therapeutic schemes involving further combinations of radiotherapy, differentiation promoter(s), and chemotherapy effectively aiming at direct or indirect tumor cell kill (e.g., by inhibiting angiogenesis) might be more appropriate. The performance of one scheme or the other may also vary according to the type of cancer to be treated, and it may be necessary to include various other features of the specific therapeutic approach(es) to be applied. Our goal was not to identify the best therapeutic option, but rather to provide a model class which is able to combine the description of the evolution of tumor cell subpopulations having different, dynamically changing phenotypes, with a large variety of therapeutic schedules, thereby explicitly accounting for stochasticity, and illustrate it for several therapy approaches, both time-discrete and continuous.

7 Assessment of future average development of tumor and normal tissue via PDEs.

In this section we want to address the problem of assessing the mean evolution of tumor and normal tissue with respect to time and to cell populations which at a specified moment in time can vary continuously in a given set of states. To this aim we deduce PDEs characterizing the dynamics of variables of interest related to the three (sub)populations of cells: CSCs, DCs, and normal cells.
We start with the SDE system obtained by coupling (1) with (12) and describing tumor and normal cell evolution in the absence of therapy:

$$dc(t) = \mu_1(c,s)dt + B_{11}(c,s)dW_1(t) + B_{12}(c,s)dW_2(t) \tag{20a}$$
$$ds(t) = \mu_2(c,s)dt + B_{21}(c,s)dW_1(t) + B_{22}(c,s)dW_2(t) \tag{20b}$$

$$dn(t) = (b_n(n) - d_n(c,s))n(t)dt + \sqrt{(b_n(n) + d_n(c,s))n(t)}dW_3(t), \tag{20c}$$

with initial conditions

$$c(t_0) = c_0, \quad s(t_0) = s_0, \quad n(t_0) = n_0, \tag{21}$$

and with the involved coefficients μ_i, B_{ij} $(i,j \in \{1,2\})$, b_n, d_n as in Subsection 2.1 and Section 5. Thereby, $W_i(t)$ $(i = 1,2,3)$ are as before mutually independent Wiener processes. Note that here t_0 is a reference time (for example, the time when the tumor was first discovered and documented, with an appropriate staging system, by a physician) and not necessarily the initiation time point of the disease. Then starting from the information available about the tumor at t_0 we want in this section to describe his future mean evolution with a PDE.
In the following we will be rather interested in characterizing the behavior of the whole tumor burden, its stemness portion, and the difference between the amount of normal tissue and the latter's critical density involving the functionality threshold γ considered in Section 5 and thus allowing to evaluate the survival chances of a patient. Therefore we consider the function $\mathbf{f} : \mathbb{R}^3 \to \mathbb{R}^3$,

$$\mathbf{f}(c_t, s_t, n_t) := (\rho_t, s_t, \vartheta_t)^t, \quad \text{where} \quad \rho_t := c_t + s_t \quad \text{and} \quad \vartheta_t := n_t - \gamma n_H.$$

Thereby n_H denotes the (constant in time) amount of normal tissue.
Let $\mathbf{X}_t := (c_t, s_t, n_t)^t$ and $\mathbf{Y}_t := (\rho_t, s_t, \vartheta_t)^t$. Then applying Itô's formula for the process $\mathbf{Y}_t = \mathbf{f}(\mathbf{X}_t)$ we get the corresponding SDE system:

$$\begin{aligned} d\mathbf{Y}_t &= \boldsymbol{\mu}(\mathbf{Y}_t)dt + \boldsymbol{\sigma}(\mathbf{Y}_t)d\mathbf{W}(t) \\ \mathbf{Y}_{t_0} &= \mathbf{y}, \end{aligned} \tag{22}$$

with the initial condition $\mathbf{y} = (c_0 + s_0, s_0, n_0 - \gamma n_H)^t$, drift $\boldsymbol{\mu}(\mathbf{Y}_t) = \begin{pmatrix} \mu_1(\mathbf{Y}_t) + \mu_2(\mathbf{Y}_t) \\ \mu_2(\mathbf{Y}_t) \\ \mu_3(\mathbf{Y}_t) \end{pmatrix}$, where $\mu_3(\mathbf{Y}_t) := \Big(b_n(Y_3(t) + \gamma n_H) - d_n(Y_1(t), Y_2(t))\Big)(Y_3(t) + \gamma n_H)$, and diffusion matrix

$$\boldsymbol{\sigma}(\mathbf{Y}_t) = \begin{pmatrix} (B_{11} + B_{21})(\mathbf{Y}_t) & (B_{12} + B_{22})(\mathbf{Y}_t) & 0 \\ B_{21}(\mathbf{Y}_t) & B_{22}(\mathbf{Y}_t) & 0 \\ 0 & 0 & \sigma(\mathbf{Y}_t) \end{pmatrix},$$

where $\sigma(\mathbf{Y}_t) := \sqrt{\Big(b_n(Y_3(t) + \gamma n_H) + d_n(Y_1(t), Y_2(t))\Big)(Y_3(t) + \gamma n_H)}$. If $(\mathbf{Y}_t)_{t \geq 0}$ is a solution to (22) on a filtered probability space $(\Omega, \mathcal{A}, \mathbb{P})$ then (see e.g. [51]) $(\mathbf{Y}_t)_{t \geq 0}$ is a Markov process relatively to that filtration, having a semigroup $(S_t)_{t \geq 0}$ defined, for any function $\boldsymbol{\phi}$ measurable and bounded on $\mathbb{R}^3$, by

$$S_t\boldsymbol{\phi}(\mathbf{y}) = \mathbb{E}[\boldsymbol{\phi}(\mathbf{Y}_t)|\mathbf{Y}_{t_0} = \mathbf{y}].$$

Its infinitesimal generator has, for any $\boldsymbol{\phi}$ twice continuously differentiable and with compact support, the form

$$\mathcal{L}\boldsymbol{\phi}(\mathbf{y}) = \sum_{i=1}^{3} \boldsymbol{\mu}_i(\mathbf{y}) \frac{\partial \boldsymbol{\phi}}{\partial y_i}(\mathbf{y}) + \frac{1}{2} \sum_{i,j=1}^{3} (\boldsymbol{\sigma}\boldsymbol{\sigma}^t)_{ij}(\mathbf{y}) \frac{\partial^2 \boldsymbol{\phi}}{\partial y_i \partial y_j}(\mathbf{y}).$$

Then (see e.g. [51]) the quantity $\mathbf{U}(t, \mathbf{y}) := \mathbb{E}[\boldsymbol{\phi}(\mathbf{Y}_t)|\mathbf{Y}_{t_0} = \mathbf{y}]$ satisfies the backward Kolmogorov PDE

$$\begin{aligned} \partial_t \mathbf{U}(t, \mathbf{y}) &= \mathcal{L}\mathbf{U}(t, \mathbf{y}) \\ \mathbf{U}(t_0, \mathbf{y}) &= \boldsymbol{\phi}(\mathbf{y}). \end{aligned}$$

This is written for convenience as a system, however, the three PDEs are actually decoupled.
Here we will choose for $\boldsymbol{\phi}$ the identity mapping on $\mathbb{R}^3$, so that we obtain for $\mathbf{U}(t, \mathbf{y}) = \mathbb{E}[\mathbf{Y}_t|\mathbf{Y}_{t_0} = \mathbf{y}]$ the system of parabolic drift-diffusion equations

$$\partial_t \mathbf{U}(t, \mathbf{y}) = \sum_{i=1}^{3} \boldsymbol{\mu}_i(\mathbf{y}) \frac{\partial \mathbf{U}}{\partial y_i}(t, \mathbf{y}) + \frac{1}{2} \sum_{i,j=1}^{3} (\boldsymbol{\sigma}\boldsymbol{\sigma}^t)_{ij}(\mathbf{y}) \frac{\partial^2 \mathbf{U}}{\partial y_i \partial y_j}(t, \mathbf{y}) \tag{23a}$$

$$\mathbf{U}(t_0, \mathbf{y}) = \mathbf{y}. \tag{23b}$$

Thus, the solution of this PDE represents the vector of expected overall tumor burden, the expected density of stem cell subpopulation, and the expected dynamic displacement from the critical functionality level of normal tissue. All these quantities depend on time and on the starting distributions of the cell populations c_0, s_0, n_0, all of which are supposed to be positive and to have finite upper bounds, say M_c, M_s and M_n, respectively. The sign of the third component of $\mathbf{U}$ can be negative or positive, according to whether the normal tissue falls or not below the critical level and it is actually an indicator of patient survival, therefore arguably more relevant than the corresponding effective amount of normal tissue. Also notice that the deduced PDE is nonautonomous with respect to the $\mathbf{y}$ variable and its divergence form is:

$$\begin{aligned}\partial_t \mathbf{U}(t,\mathbf{y}) &= \sum_{i,j=1}^{3}\Big(\frac{1}{2}(\boldsymbol{\sigma}\boldsymbol{\sigma}^t)_{ij}(\mathbf{y})\frac{\partial \mathbf{U}}{\partial y_i}(t,\mathbf{y})\Big)_{y_j} + \sum_{i=1}^{3}\Big(\boldsymbol{\mu}_i(\mathbf{y}) - \frac{1}{2}\sum_{j=1}^{3}\frac{\partial(\boldsymbol{\sigma}\boldsymbol{\sigma}^t)_{ij}}{\partial y_j}(\mathbf{y})\Big)\frac{\partial \mathbf{U}}{\partial y_i}(t,\mathbf{y}) \qquad (24a)\\ &= \operatorname{div}(\frac{1}{2}\boldsymbol{\sigma}\boldsymbol{\sigma}^t\nabla\mathbf{U}(t,\mathbf{y})) + \Big(\boldsymbol{\mu} - \frac{1}{2}\operatorname{div}(\boldsymbol{\sigma}\boldsymbol{\sigma}^t)\Big)\cdot\nabla\mathbf{U}(t,\mathbf{y})\\ \mathbf{U}(t_0,\mathbf{y}) &= \mathbf{y}. \qquad (24b)\end{aligned}$$

Alternatively a backward problem with terminal condition can be obtained (see e.g. [51]) by considering

$$\mathbf{u}(\tau,\mathbf{y}) := \mathbb{E}[\mathbf{Y}_T|\mathbf{Y}_\tau = \mathbf{y}], \quad t_0 \le \tau \le T, \qquad (25)$$

with $\mathbf{y}$ in $D := \mathbb{R}^3_+$, which satisfies the final value problem

$$\begin{aligned}\partial_\tau \mathbf{u}(\tau,\mathbf{y}) + \sum_{i=1}^{3}\boldsymbol{\mu}_i(\mathbf{y})\frac{\partial \mathbf{u}}{\partial y_i}(\tau,\mathbf{y}) + \frac{1}{2}\sum_{i,j=1}^{3}(\boldsymbol{\sigma}\boldsymbol{\sigma}^t)_{ij}(\mathbf{y})\frac{\partial^2 \mathbf{u}}{\partial y_i \partial y_j}(\tau,\mathbf{y}) = \mathbf{0} \quad \text{in } (t_0,T)\times D \qquad (26a)\\ \mathbf{u}(T,\mathbf{y}) = \mathbf{y} \quad \text{in } D, \qquad (26b)\end{aligned}$$

together with boundary conditions like those mentioned above. Equation (25) defines the expectations of the quantities of interest ρ_t, s_t, ϑ_t (overall tumor burden, density of stem cells, and dynamic displacement from the critical functionality level of normal tissue) at some later time T provided they were known at some earlier time τ. In our context, the latter could be the time of diagnosis (usually differing from patient to patient) and T could correspondingly represent the follow-up time. Note that (26) can be reduced to the class of PDEs of type (23) by the transformation $\mathbf{U}(T + t_0 - \tau, \mathbf{y}) := \mathbf{u}(\tau, \mathbf{y})$.
Including therapeutic effects can be easily done for continuously applied therapies, as in the SDE framework we accounted for such effects by way of the coefficients in the SDEs involving birth, death, and transition rates affected by the respective therapeutic agent. Time-discrete therapies with ionizing radiation applied at discrete, pre-specified times can be described in this context similar to what we did in Subsection 3.4, i.e. using some stochastic processes L_t to characterize the cumulative treatment effect on the quantities given by the components of the vector $\mathbf{U}(t,\mathbf{y})$ (or for that matter $\mathbf{u}(T + t_0 - t, \mathbf{y})$) determined by solving the above initial (or, correspondingly, terminal)-boundary value problem. For instance, instead of (9) we could consider

$$R_\rho(t,\mathbf{y}) = (U_1 - U_2)(t,\mathbf{y})e^{-\varepsilon_c L_t^{(c)}} + U_2(t,\mathbf{y})e^{-\varepsilon_s L_t^{(s)}}, \quad R_s(t,\mathbf{y}) = U_2(t,\mathbf{y})e^{-\varepsilon_s L_t^{(s)}},$$

with $L_t^{(c)}$ and $L_t^{(s)}$ as in Subsection 3.4 and use these to dynamically replace the initial conditions for U_1 and U_2 on every new computed time interval. We only describe the concept here and address explicitly merely the case without therapy in order not to overload the presentation.

7.1 Numerical simulations

System (24) involves three PDEs, each of the solution components depending on time and on a three-dimensional vector $\mathbf{y}$. However, taking a closer look at the original SDE system (20) we see that the third equation is decoupled from the first two. This observation can help to reduce the computational effort needed for solving (24). Indeed, similarly with what we did above, we can write a PDE system for $\tilde{\mathbf{U}}(t,\tilde{\mathbf{y}}) = (U_1(t,\tilde{\mathbf{y}}), U_2(t,\tilde{\mathbf{y}}))^t$, where $\tilde{\mathbf{y}} = (y_1, y_2)^t$:

$$\partial_t \tilde{\mathbf{U}}(t,\tilde{\mathbf{y}}) = \sum_{i,j=1}^{2}\Big(\frac{1}{2}(\tilde{\boldsymbol{\sigma}}\tilde{\boldsymbol{\sigma}}^t)_{ij}(\tilde{\mathbf{y}})\frac{\partial \tilde{\mathbf{U}}}{\partial \tilde{y}_i}(t,\tilde{\mathbf{y}})\Big)_{\tilde{y}_j} + \sum_{i=1}^{2}\Big(\tilde{\boldsymbol{\mu}}_i(\tilde{\mathbf{y}}) - \frac{1}{2}\sum_{j=1}^{2}\frac{\partial(\tilde{\boldsymbol{\sigma}}\tilde{\boldsymbol{\sigma}}^t)_{ij}}{\partial \tilde{y}_j}(\tilde{\mathbf{y}})\Big)\frac{\partial \tilde{\mathbf{U}}}{\partial \tilde{y}_i}(t,\tilde{\mathbf{y}}) \qquad (27a)$$

$$= \operatorname{div}(\frac{1}{2}\tilde{\sigma}\tilde{\sigma}^t\nabla\mathbf{U}(t,\tilde{\mathbf{y}})) + \Big(\tilde{\mu} - \frac{1}{2}\operatorname{div}(\tilde{\sigma}\tilde{\sigma}^t)\Big)\cdot\nabla\tilde{\mathbf{U}}(t,\tilde{\mathbf{y}}) \quad \text{in } (t_0,T)\times\mathbb{R}^2_+,$$

$$\tilde{\mathbf{U}}(t_0,\tilde{\mathbf{y}}) = \tilde{\mathbf{y}} \quad \text{in } \mathbb{R}^2_+, \tag{27b}$$

where we will only compute the solution on the domain $\tilde{D} = (0, M_c + M_s)\times(0, M_s)$. In the above equations

$$\tilde{\mu}(\tilde{\mathbf{y}}) = \begin{pmatrix} \mu_1(\tilde{\mathbf{y}}) + \mu_2(\tilde{\mathbf{y}}) \\ \mu_2(\tilde{\mathbf{y}}) \end{pmatrix}, \qquad \tilde{\sigma}(\tilde{\mathbf{y}}) = \begin{pmatrix} (B_{11}+B_{21})(\tilde{\mathbf{y}}) & (B_{12}+B_{22})(\tilde{\mathbf{y}}) \\ B_{21}(\tilde{\mathbf{y}}) & B_{22}(\tilde{\mathbf{y}}) \end{pmatrix}. \tag{28}$$

This system of decoupled, linear PDEs is nonautonomous with respect to the two-dimensional $\tilde{\mathbf{y}}$ variable and can be solved to provide at any time the expected total tumor burden and the expected amount of stem cells in that tumor.
To determine the quantity $U_3(t,\mathbf{y}) = \mathbb{E}[Y_3(t,\tilde{\mathbf{y}})|Y_3(t_0) = y_3]$ we need the full vector $\mathbf{y}$, thus the corresponding scalar PDE will have to be solved in 3D:

$$\partial_t U_3(t,\mathbf{y}) = \mu_3(\mathbf{y})\frac{\partial U_3}{\partial y_3}(\mathbf{y}) + \frac{1}{2}\sigma^2(\mathbf{y})\frac{\partial^2 U_3}{\partial y_3^2}(\mathbf{y}) \quad \text{in } (t_0,T)\times\mathbb{R}^3 \tag{29a}$$

$$U_3(t_0,\mathbf{y}) = y_3 \quad \text{in } \mathbb{R}^3. \tag{29b}$$

The solution will be computed on $D = \tilde{D}\times(-\gamma n_H, M_n - \gamma n_H)$. We use a Douglas-Rachford alternating direction (ADI) finite difference method which makes one dimension implicit at each time step, while leaving the other two dimensions explicit. Here a more accurate ADI scheme (see [14]) has been implemented and employed to find the approximations of the solution components. The parameters involved in the coefficients of the PDEs are the same as those used in Sections 2 and 5. Figure 15 shows the solution components at different times: U_1: expected total tumor burden, U_2: expected amount of tumor stem cells, and U_3: expected deviation of normal cells/tissue from the critical level at which the affected region is still functional. The latter was taken to be $\gamma = 0.7$, i.e. 70% of the normal cells have to be preserved in order to ensure tissue functionality. Notice that with time passing the normal tissue is more and more degraded, as a consequence of the interaction with tumor cells. Increasing the functionality threshold drives U_3 into the negative region, meaning that patient survival chances are dramatically impaired. Such a situation is illustrated in Figure 16, where $\gamma = 0.85$, while the rest of the parameters remain unchanged. Only U_3 is represented, as U_1 and U_2 do not change with γ due to the normal cells not influencing the evolution of tumor cells.

7.2 Analytical approximations based on Euler SDE discretization

In this subsection we describe a way to derive closed-form analytical approximations of the predicted mean of $\mathbf{Y}_T$ based on the staging of the tumor at τ, i.e. for $\mathbf{u}(\tau,\mathbf{y}) = \mathbb{E}[\mathbf{Y}_T|\mathbf{Y}_\tau = \mathbf{y}]$ with $\tau\in[t_0,T]$ and $\mathbf{y}\in\mathbb{R}^3_+$. However, in order to simplify the presentation we will only illustrate the method for the vector of the first two components u_1, u_2, hence corresponding to the solution of the PDE system

$$\partial_\tau\tilde{\mathbf{u}}(\tau,\tilde{\mathbf{y}}) + \sum_{i=1}^{2}\tilde{\mu}_i(\tilde{\mathbf{y}})\frac{\partial\tilde{\mathbf{u}}}{\partial\tilde{y}_i}(\tau,\tilde{\mathbf{y}}) + \frac{1}{2}\sum_{i,j=1}^{2}(\tilde{\sigma}\tilde{\sigma}^t)_{ij}(\tilde{\mathbf{y}})\frac{\partial^2\tilde{\mathbf{u}}}{\partial\tilde{y}_i\partial\tilde{y}_j}(\tau,\tilde{\mathbf{y}}) = \mathbf{0} \quad \text{in } (t_0,T)\times\mathbb{R}^2_+ \tag{30a}$$

$$\tilde{\mathbf{u}}(T,\tilde{\mathbf{y}}) = \tilde{\mathbf{y}} \quad \text{in } \mathbb{R}^2_+, \tag{30b}$$

where t_0 represents the initiation time of the tumor. For simplicity of notation we will omit the tildes on the variables in the following, but always mean the 2D vectors, unless otherwise stated. In the following we give an analytical approximation of the solution to (30) on a small prediction interval (τ,T).[5] The idea presented here can be recursively extended such that the corresponding results hold on an arbitrary prediction interval (τ,T), however, they would have a very cumbersome closed form.

Proposition 7.1 *Let* $\mathbf{z} := (\ln y_1, \ln y_2)^t$, $\mathbf{y} := (y_1,y_2)\in\mathbb{R}^2_+$. *Then an analytical approximation of the solution to* (30) *on a small prediction interval* (τ,T) *is given componentwise by*

$$u_j(\tau,\mathbf{y}) \simeq E_{AS}(\mathbf{M}(\mathbf{z}))\Bigg[\mathcal{I}_j(\mathbf{z})\Big(\eth\nabla A_j(\mathbf{M}(\mathbf{z})) + \frac{1}{2}\nabla S_{jj}(\mathbf{M}(\mathbf{z}))\Big)\cdot\mathbf{S}_{\cdot j}(\mathbf{z})$$

[5] By small interval is meant e.g. an interval of length $2\eth$, where $\eth$ is the discretization step of the Euler scheme for the SDE system (22).

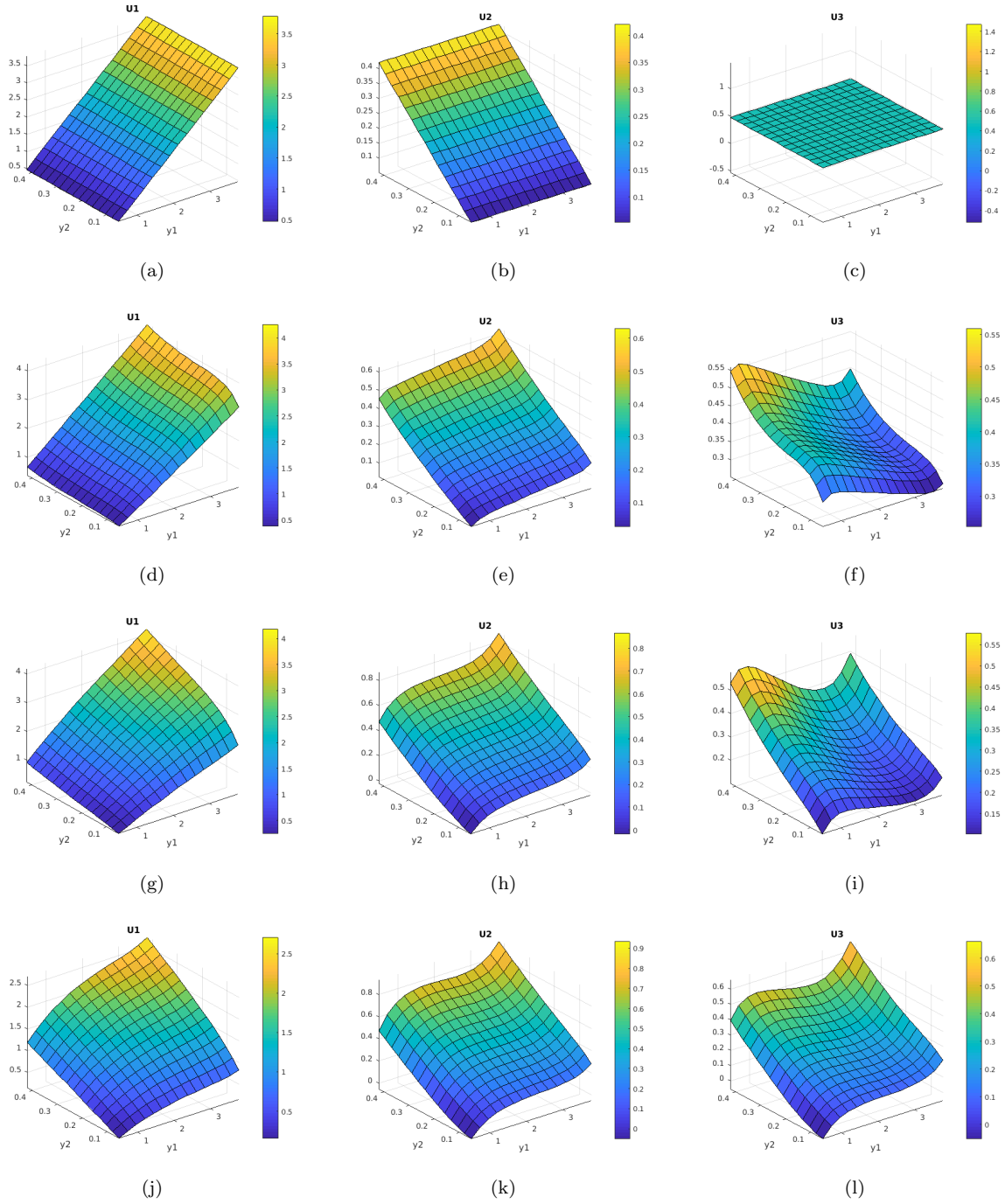

Figure 15: Solution components of (27) and (29) at various time moments, no therapy applied. Left column: expected total tumor burden, middle: expected density of cancer stem cells, right: expected deviations of normal cells from critical threshold for which $\gamma = 0.7$. Plots 15(a)-15(c): initial state, 15(d)-15(f): 10 days, 15(g)-15(i): 30 days, 15(j)-15(l): 70 days.

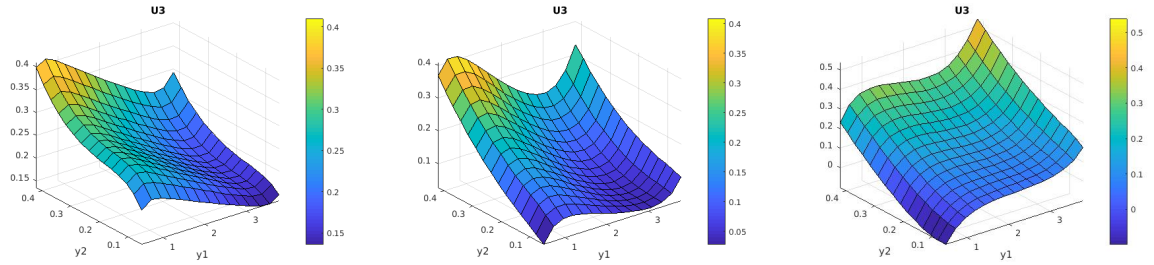

(a) (b) (c)

Figure 16: Solution of (29) at different times, with no therapy applied. Shown are expected deviations of normal cells from the critical threshold for which $\gamma = 0.85$. Plot 16(a): 10 days, 16(b): 30 days, 16(c): 70 days.

$$+\Big(\frac{\eth}{2}\operatorname{Hess} A_j(\mathbf{M}(\mathbf{z})) + \frac{1}{4}\operatorname{Hess} S_{jj}(\mathbf{M}(\mathbf{z}))\Big) : \boldsymbol{\mathcal{M}}_2^j(\mathbf{z})\Big],$$

where $j = 1, 2$ and we used the following notations ($\boldsymbol{\zeta} \in \mathbb{R}^2$):

$$\mathbf{A}(\boldsymbol{\zeta}) := \begin{pmatrix} e^{-\zeta_1}(\tilde{\mu}_1(\boldsymbol{\zeta}) + \tilde{\mu}_2(\boldsymbol{\zeta})) - \frac{1}{2}e^{-2\zeta_1}(\tilde{\sigma}_{11}^2(\boldsymbol{\zeta}) + \tilde{\sigma}_{12}^2(\boldsymbol{\zeta})) \\ e^{-\zeta_2}\tilde{\mu}_2(\boldsymbol{\zeta}) - \frac{1}{2}e^{-2\zeta_2}(\tilde{\sigma}_{21}^2(\boldsymbol{\zeta}) + \tilde{\sigma}_{22}^2(\boldsymbol{\zeta})) \end{pmatrix}, \tag{31}$$

$$\mathbf{M}(\boldsymbol{\zeta}) := \boldsymbol{\zeta} + \mathbf{A}(\boldsymbol{\zeta})\eth, \qquad \boldsymbol{\Sigma}(\boldsymbol{\zeta}) := \begin{pmatrix} e^{-\zeta_1}\tilde{\sigma}_{11}(\boldsymbol{\zeta}) & e^{-\zeta_1}\tilde{\sigma}_{12}(\boldsymbol{\zeta}) \\ e^{-\zeta_2}\tilde{\sigma}_{21}(\boldsymbol{\zeta}) & e^{-\zeta_2}\tilde{\sigma}_{22}(\boldsymbol{\zeta}) \end{pmatrix}, \quad \mathbb{S}(\boldsymbol{\zeta}) := \eth\boldsymbol{\Sigma}(\boldsymbol{\zeta}) \tag{32}$$

$$E_{AS}(\boldsymbol{\zeta}) := \exp\Big(\eth\boldsymbol{\delta}_j \cdot \mathbf{A}(\boldsymbol{\zeta}) + \frac{1}{2}\boldsymbol{\delta}_j^t\mathbb{S}(\boldsymbol{\zeta})\boldsymbol{\delta}_j\Big),$$

$$\mathcal{I}_j(\boldsymbol{\zeta}) := \exp\Big(\boldsymbol{\delta}_j \cdot \mathbf{M}(\boldsymbol{\zeta}) + \frac{1}{2}\boldsymbol{\delta}_j^t\mathbb{S}(\boldsymbol{\zeta})\boldsymbol{\delta}_j\Big),$$

$$(\boldsymbol{\mathcal{M}}_2^j(\boldsymbol{\zeta}))_{km} := \mathcal{I}_j(\boldsymbol{\zeta})\Big(S_{jm}(\boldsymbol{\zeta})S_{jk}(\boldsymbol{\zeta}) + S_{km}(\boldsymbol{\zeta})\Big),$$

$$\boldsymbol{\delta}_j := (\delta_{j1}, \delta_{j2})^t, \text{ where } \delta_{ij} \text{ is the usual Kronecker symbol, } \eth := \frac{T-\tau}{2}.$$

Thereby, $\tilde{\mu}$ and $\tilde{\sigma}$ are as in (28), $\mathbf{S}_{\cdot j}$ denotes the column j of $\mathbb{S}$, and as usual $A : B = trace(AB^t)$ for A, B arbitrary matrices.

Proof: Let $Z_j(\tau) := \ln Y_j(\tau)$, $j = 1, 2$. Then $u_j(\tau, \mathbf{y}) = \mathbb{E}[e^{Z_j(T)}|Z_1(\tau) = \ln y_1, Z_2(\tau) = \ln y_2]$. The SDE system satisfied by $\mathbf{Z} = (Z_1, Z_2)^t$ reads

$$d\mathbf{Z}_t = \mathbf{A}(\mathbf{Z}_t)dt + \boldsymbol{\Sigma}(\mathbf{Z}_t)d\mathbf{W}(t), \tag{33a}$$

$$\mathbf{Z}_\tau = \mathbf{z}, \qquad t \in [\tau, T], \tag{33b}$$

where $\mathbf{z} = (\ln y_1, \ln y_2)^t$, and the drift and diffusion coefficients $\mathbf{A}(\mathbf{Z}_t)$ and $\boldsymbol{\Sigma}(\mathbf{Z}_t)$ are those given in (31) and (32), respectively. In general, the discretization of (33) has the form

$$\mathbf{Z}_{\tau_{k+1}} = \mathbf{Z}_{\tau_k} + \mathbf{A}(\mathbf{Z}_{\tau_k})\eth + \boldsymbol{\Sigma}(\mathbf{Z}_{\tau_k})\sqrt{\eth}\boldsymbol{\varepsilon}_k, \quad \boldsymbol{\varepsilon}_k \sim N(\mathbf{0}, \mathbb{I}_2), \quad k = 0, \dots, n-1, \tag{34}$$

where $\tau = \tau_0 < \tau_1 < \cdots < \tau_n = T$ and $\eth = \tau_{k+1} - \tau_k = \frac{T-\tau}{n}$.
We aim at computing the approximation

$$\mathbb{E}[e^{Z_j(T)}|\mathbf{Z}(\tau) = \mathbf{z}] \simeq \int_{\mathbb{R}^2} e^{z_j^{(n)}} p_{\tau,T}(\mathbf{z}^{(n)}|\mathbf{z}^{(0)})d\mathbf{z}^{(n)}, \tag{35}$$

where $\mathbf{z}^{(0)} = \mathbf{z}$ and $p_{\tau,T}$ is the transition density from τ to T for the Markov process given in (34). Between such transition densities it is well known that we have the following representation:

$$p_{\tau_0,\tau_n}(\mathbf{z}^{(n)}|\mathbf{z}^{(0)}) = \int_{\mathbb{R}^2}\cdots\int_{\mathbb{R}^2} p_{\tau_0,\tau_1}(\mathbf{z}^{(1)}|\mathbf{z}^{(0)})p_{\tau_1,\tau_2}(\mathbf{z}^{(2)}|\mathbf{z}^{(1)})\dots p_{\tau_{n-1},\tau_n}(\mathbf{z}^{(n)}|\mathbf{z}^{(n-1)})\, d\mathbf{z}^{(1)}\dots d\mathbf{z}^{(n)} \tag{36}$$

and consider that $p_{\tau_k,\tau_{k+1}}(\mathbf{z}^{(k+1)}|\mathbf{z}^{(k)})$ is the density of a normal distribution of mean $\mathbf{M}(\mathbf{z}^{(k)})$ and variance $\mathbb{S}(\mathbf{z}^{(k)})$ according to (32), thus

$$p_{\tau_k,\tau_{k+1}}(\mathbf{z}^{(k+1)}|\mathbf{z}^{(k)}) = \frac{1}{2\pi(\det \mathbb{S}(\mathbf{z}^{(k)}))^{1/2}} \exp\Big(-\frac{1}{2}(\mathbf{z}^{(k+1)} - \mathbf{M}(\mathbf{z}^{(k)}))^t \mathbb{S}^{-1}(\mathbf{z}^{(k)})(\mathbf{z}^{(k+1)} - \mathbf{M}(\mathbf{z}^{(k)}))\Big),$$

for all $\mathbf{z}^{(k+1)} \in \mathbb{R}^2$, $k = 0, \dots, n-1$.
To compute (35) recall that we consider for the sake of clarity $n = 2$; the computations for the more general case are analogous, but more tedious.

$$\begin{aligned}\mathbb{E}[e^{Z_j(T)}|\mathbf{Z}(\tau) = \mathbf{z}] &\simeq \int_{\mathbb{R}^2} e^{z_j^{(2)}} \int_{\mathbb{R}^2} p_{\tau_0,\tau_1}(\mathbf{z}^{(1)}|\mathbf{z}^{(0)}) p_{\tau_1,\tau_2}(\mathbf{z}^{(2)}|\mathbf{z}^{(1)})\ d\mathbf{z}^{(1)} d\mathbf{z}^{(2)} \\ &= \int_{\mathbb{R}^2} p_{\tau_0,\tau_1}(\mathbf{z}^{(1)}|\mathbf{z}^{(0)}) \int_{\mathbb{R}^2} e^{z_j^{(2)}} p_{\tau_1,\tau_2}(\mathbf{z}^{(2)}|\mathbf{z}^{(1)})\ d\mathbf{z}^{(2)}\ d\mathbf{z}^{(1)}. \end{aligned} \tag{37}$$

To calculate the inner integral in (37) observe that it is the Laplace transform of a multivariate normal density. Denoting $\boldsymbol{\delta}_j := (\delta_{j1}, \delta_{j2})^t$, where δ_{ij} is the usual Kronecker symbol, we can write

$$\begin{aligned}\int_{\mathbb{R}^2} e^{z_j^{(2)}} p_{\tau_1,\tau_2}(\mathbf{z}^{(2)}|\mathbf{z}^{(1)})\ d\mathbf{z}^{(2)} &= \int_{\mathbb{R}^2} e^{\boldsymbol{\delta}_j \cdot \mathbf{z}^{(2)}} p_{\tau_1,\tau_2}(\mathbf{z}^{(2)}|\mathbf{z}^{(1)})\ d\mathbf{z}^{(2)} \\ &= \exp\Big(\boldsymbol{\delta}_j \cdot \mathbf{M}(\mathbf{z}^{(1)}) + \frac{1}{2}\boldsymbol{\delta}_j^t \mathbb{S}(\mathbf{z}^{(1)})\boldsymbol{\delta}_j\Big).\end{aligned}$$

Plugging this into (37) gives

$$\mathbb{E}[e^{Z_j(T)}|\mathbf{Z}(\tau) = \mathbf{z}] \simeq \int_{\mathbb{R}^2} \exp\Big(\boldsymbol{\delta}_j \cdot (\mathbf{z}^{(1)} + \eth \mathbf{A}(\mathbf{z}^{(1)})) + \frac{1}{2}\boldsymbol{\delta}_j^t \mathbb{S}(\mathbf{z}^{(1)})\boldsymbol{\delta}_j\Big) p_{\tau_0,\tau_1}(\mathbf{z}^{(1)}|\mathbf{z}^{(0)})\ d\mathbf{z}^{(1)}. \tag{38}$$

We expand the exponential of the nonlinear part from the above integral in a Taylor series of second order around the point $\mathbf{M}(\mathbf{z}^{(0)})$,[6] then use the Laplace transform for a multivariate normal distribution to assess the terms of the form

$$\begin{aligned}\int_{\mathbb{R}^2} e^{\boldsymbol{\lambda}\cdot\mathbf{z}^{(1)}} z_r^{(1)} p_{\tau_0,\tau_1}(\mathbf{z}^{(1)}|\mathbf{z}^{(0)})\ d\mathbf{z}^{(1)} &= \frac{\partial}{\partial\lambda_r} \exp\Big(\boldsymbol{\lambda}\mathbf{M}(\mathbf{z}^{(0)}) + \frac{1}{2}\boldsymbol{\lambda}^t \mathbb{S}(\mathbf{z}^{(0)})\boldsymbol{\lambda}\Big), \qquad r = 1, 2 \\ \int_{\mathbb{R}^2} e^{\boldsymbol{\lambda}\cdot\mathbf{z}^{(1)}} z_r^{(1)} z_s^{(1)} p_{\tau_0,\tau_1}(\mathbf{z}^{(1)}|\mathbf{z}^{(0)})\ d\mathbf{z}^{(1)} &= \frac{\partial^2}{\partial\lambda_r\partial\lambda_s} \exp\Big(\boldsymbol{\lambda}\mathbf{M}(\mathbf{z}^{(0)}) + \frac{1}{2}\boldsymbol{\lambda}^t \mathbb{S}(\mathbf{z}^{(0)})\boldsymbol{\lambda}\Big), \qquad r, s = 1, 2.\end{aligned}$$

These calculations lead to

$$\begin{aligned}\mathcal{M}_{1,r}(\mathbf{z}^{(0)}) &:= \int_{\mathbb{R}^2} e^{\boldsymbol{\delta}_j\cdot\mathbf{z}^{(1)}} z_r^{(1)}\ p_{\tau_0,\tau_1}(\mathbf{z}^{(1)}|\mathbf{z}^{(0)})\ d\mathbf{z}^{(1)} \\ &= \exp\Big(\boldsymbol{\delta}_j \cdot \mathbf{M}(\mathbf{z}^{(0)}) + \frac{1}{2}\boldsymbol{\delta}_j^t \mathbb{S}(\mathbf{z}^{(0)})\boldsymbol{\delta}_j\Big)\Big(M_r(\mathbf{z}^{(0)}) + S_{jr}(\mathbf{z}^{(0)})\Big), \quad j, r = 1, 2 \\ \mathcal{M}_{2,rs}(\mathbf{z}^{(0)}) &:= \mathcal{M}_{1,r}(\mathbf{z}^{(0)})(M_r(\mathbf{z}^{(0)}) + S_{jr}(\mathbf{z}^{(0)})) + S_{sr}(\mathbf{z}^{(0)}) \exp\Big(\boldsymbol{\delta}_j \cdot \mathbf{M}(\mathbf{z}^{(0)}) + \frac{1}{2}\boldsymbol{\delta}_j^t \mathbb{S}(\mathbf{z}^{(0)})\boldsymbol{\delta}_j\Big),\end{aligned}$$

$j, r, s = 1, 2$. Replacing into (38) gives the claim, after rewriting the obtained formula with the aid of matrix-vector multiplications. □

8 Conclusions and outlook

Noise is an important component of all physiological processes. In cancer development and treatment it plays an important role, too, as there is a large patient-to-patient variability concerning both the evolution of a tumor and its response to therapy. Moreover, cell population reduction effected by therapy leads to small cell numbers and thus to fluctuations. In this work we proposed a modeling approach involving SDEs and obtained from simple transition probabilities, thereby paying particular attention to the deduction of the SDEs. The explicit drift and diffusion terms are derived from step-by-step modeling and not by simply adding some multiplicative noise to an ODE system describing in a more or less heuristic

[6] Actually a Taylor expansion of any order can be used and all computations can be performed explicitly in an absolutey analogous way, however they can become very involved, therefore we restrain here to this second order expansion.

way the evolution of the tumor cell subpopulations. For instance, the form of the (negative) diffusion coefficients for the model in [49] is largely arbitrary and needs justification. The same applies to the simple multiplicative form of (positive) diffusions in the models from [52, 65]. We would like, however, to mention here the model in [56] focusing on another issue related to tumor growth and effectively deducing the coefficients of the corresponding single SDE by a diffusion limit of branching processes. The deduction method we used here is related to that in [56] and similar to what has been done in [2] for an SDE system characterizing the dynamics of interacting populations, however with relevant modifications aiming at preserving the positivity of solutions. Indeed, the conditions for the latter were shown in [10] to be necessary and sufficient, therefore they actually guided the modeling, in particular by requiring some of the mitotic and differentiation rates to be nonconstant.

Further factors from the tumor microenvironment, e.g., tumor acidity, affect cell proliferation, differentiation, and therapeutic response of both normal and neoplastic tissues. Such effects can be included by considering a supplementary (deterministic or stochastic) equation for the dynamics of proton concentration and modifying the cell splitting rates to let them depend not just on the available amount of cells, but also on the acidity. Birth and death rates could depend on the latter as well. An SDE system with correlated Wiener processes would be more realistic, but also more challenging, as the theory and numerics of such systems still have to be developed for the situation where the SDEs are coupled in such nonlinear way as is the case here.

Even for a nonlinear SDE system like ours, with independent Brownian motions characterizing the noise there are still enough open problems: The solutions can be shown to exist only locally, the numerical schemes available so far are not positivity preserving, and, moreover, the system can become stiff when small cell densities are reached simultaneously in both subpopulations, leading to large diffusion coefficients needing to be balanced by a tiny discretization step.

Passing to a PDE system like in Section 7 enables accounting for the (expected) evolution of tumor cells in interaction with the surrounding normal tissue not only with respect to time, but also depending on continuous ranges of tumor and (shifted) normal cell densities, so that predictions become available for different scenarios of the tumor and normal tissue states, thereby also making allowance for tumor heterogeneity with respect to stemness. Similarly, other cell phenotypes can be considered in this modeling framework, e.g. if one is interested in the migratory (mesenchymal vs. amoeboid, moving vs. proliferating, etc.) behavior of tumor cells in order to assess not just growth, but also spread of the neoplastic tissue. Indeed, besides time evolution the space dynamics also plays an essential role in the assessment of several indicators of tumor malignancy, among others acidity, cell motility, and tissue degradation. In particular, radiotherapy needs a correct estimation of tumor margins for determining the CTV/PTV[7]. For instance, this issue is of outmost relevance for cancers like glioma, whose spread heavily relies on the underlying, highly anisotropic and patient-specific brain tissue structure. Accounting for such effects leads to systems of partial differential equations of reaction-diffusion-taxis type, some coupled to ODEs. Accounting for stochasticity in that context is far more challenging, and even with major simplifications there are but few references addressing such models. They involve PDEs with random coefficients [29, 30] or couplings between PDEs and SDEs [28, 38]. The latter, however, only take into account a single cancer cell population moving and proliferating under the influence of intra- and extracellular tumor acidity, and were obtained in a heuristic way. Effectively deducing adequate coupled PDEs from transition probabilities for interacting cell subpopulations inferring phenotypic switch triggered by randomly influenced population densities or just by some external factors would be a most interesting, but also challenging issue even if only done formally.

Still in the present framework of interacting cell populations just depending on time, the issue of cancer stem cell plasticity in which tumor cells harbor the dynamic ability of shifting from a non-CSC state to a CSC state and back gives rise to more complicated two-way couplings, therefore we made here the simplifying assumption that CSCs only divide symmetrically or asymmetrically and cannot arise from differentiated cells. Including CSC plasticity can be, however, of substantial relevance to the therapeutic outcome [42] and as such deserves investigation. Mathematical models have the great advantage of being amply versatile and allowing to test a large variety of approaches with features which can be turned on and off at will in the simulations. Therefore, they have the potential of helping to understand both the modeled processes and the performance of the therapeutic approach.

[7] CTV: clinical target volume, PTV: planning target volume

9 Appendix

9.1 Recalling invariance criteria for SDEs

In this appendix we recall the result of [10] concerning stochastic invariance.
Let $(\Omega, \mathcal{F}, \mathbb{P})$ be a probability space with a right-continuous increasing family $F = (\mathcal{F}_t)_{t\geq 0}$ of sub-σ fields of $\mathcal{F}$, each containing all sets of $\mathbb{P}$-measure zero. We consider an SDE system of the form

$$\begin{aligned} dX(t) &= f(t, X(t))dt + g(t, X(t))dW(t), \quad t \in (0, \infty), \\ X(0) &= X_0, \end{aligned} \tag{39}$$

where $f : [0, \infty) \times \mathbb{R}^m \to \mathbb{R}^m$ and $g : [0, \infty) \times \mathbb{R}^m \to \mathbb{R}^{m\times r}$ are locally Lipschitz continuous in the X-argument and continuous w.r.t. t, whereas $W : [0, \infty) \times \Omega \to \mathbb{R}^r$ is an r- dimensional F- adapted Wiener process.

Definition 9.1 ([10]) *The subset $K \subset \mathbb{R}^m$ is called* invariant *for the system* (39) *if for every $X_0 \in K$ the corresponding solution $(X(t))_{t\geq 0}$ satisfies*

$$P(\{X(t) \in K,\ t \in (0, \infty)\}) = 1.$$

Theorem 9.1 ([10]) *Let $I \subset \{1, \ldots, m\}$ be non-empty. Then the set*

$$K := \{x \in \mathbb{R}^m \ :\ x_i \geq 0,\ i \in I\}$$

is invariant for the stochastic system (39) *if and only if*

$$\begin{aligned} f_i(t, x) &\geq 0 \quad \text{for } x \in K \text{ s.t. } x_i = 0, \\ g_{ij}(t, x) &= 0 \quad \text{for } x \in K \text{ s.t. } x_i = 0,\ j = 1, \ldots, r \end{aligned}$$

for all $t \geq 0$ and $i \in I$.

Acknowledgement

JMK is supported by the Basque Government through the BERC 2018- 2021 program and by the Spanish State Research Agency through BCAM Severo Ochoa excellence accreditation SEV-2017-0718 and through project RTI2018- 093416-B-I00 funded by (AEI/FEDER, UE) and acronym MULTIQUANT. CS acknowledges the support of the Federal Ministry of Education and Research BMBF in the project GlioMaTh-05M16UKB. The authors would like to thank Pawan Kumar (TU Kaiserslautern) for helping with the implementation of the ADI finite difference scheme used in Subsection 7.1. We also thank our reviewers, whose comments were very helpful in improving this work.

References

[1] A. Agren, A. Brahme, and I. Turesson. Optimization of uncomplicated control for head and neck tumors. *Int. J. Radiology Oncology Biol. Phys.*, 19:1077–1085, 1990.

[2] E. Allen. *Modeling with Itô Stochastic Differential Equations*. Mathematical Modelling: Theory and Applications. Springer, 2007.

[3] S. Bao, Q. Wu, R.E. McLendon, and Y. et al. Hao. Glioma stem cells promote radioresistance by preferential activation of the DNA damage response. *Nature*, 444:756 – 760, 2006.

[4] A. Barrett, J. Dobbs, S. Morris, and T. Roques. *Practical Radiotherapy Planning*. Hodder Arnold, 2009, 4th edition.

[5] E. Beretta, V. Capasso, and N. Morozova. Mathematical modeling of cancer stem cells population behavior. *Mat. Model. Nat. Phenom.*, 7:279 – 305, 2012.

[6] J. Bernier, C. Domenge, and M. et al. Ozsahin. Postoperative irradiation with or without concomitant chemotherapy for locally advanced head and neck cancer. *N. Engl. J. Med.*, 350:1945–1952, 2004.

[7] M.U. Bogdanska, M. Bodnar, M.J. Piotrowska, M. Murek, P. Schucht, J. Beck, A. Martinez-Gonzalez, and V.M. Perez-Garcia. A mathematical model describes the malignant transformation of low grade gliomas: Prognostic implications. *PLoS ONE*, 12:e0179999, 2017.

[8] K.N. Chadwick and H.P. Leenhouts. *The Molecular Theory of Radiation Biology*. Springer, 1981.

[9] Der-Yang Cho, Shinn-Zong Lin, Wen-Kuang Yang, Han-Chung Lee, Den-Mei Hsu, Hung-Lin Lin, Chun-Chung Chen, Chun-Lin Liu, Wen-Yuan Lee, and Li-Hui Ho. Targeting cancer stem cells for treatment of glioblastoma multiforme. *Cell Transplantation*, 22(4):731–739, 2013.

[10] J. Cresson and S. Sonner. A note on a derivation method for sde models: Applications in biology and viability criteria. *Stoch. Anal. Appl.*, 36:224–239, 2018.

[11] A. Dawson and T. Hillen. Derivation of the tumor control probability (tcp) from a cell cycle. *Computational and Mathematical Methods in Medicine*, 7(2-3):121–141, June-September 2006.

[12] J.E. Dick. Stem cell concepts renew cancer research. *Blood*, 112:4793–4807, 2008.

[13] D. Dingli and F. Michor. Successful therapy must eradicate cancer stem cells. *Stem Cells*, 24:2603 – 2610, 2006.

[14] J. Douglas. Alternating direction methods for three space variables. *Numer. Math.*, 4:41–63, 1962.

[15] T. Eckschlager, J. Plch, M. Stiborova, and J. Hrabeta. Histone deacetylase inhibitors as anticancer drugs. *Int. J. Molec. Sci.*, 18:1414, 2017.

[16] H. Enderling, L. Hlatky, and P. Hahnfeldt. Migration rules: tumours are conglomerates of self-metastases. *Br. J. Cancer*, 100:1917–1925, 2009.

[17] H. Enderling, L. Hlatky, and P. Hahnfeldt. Cancer stem cells: A minor cancer subpopulation that redefines global cancer features. *Front. Oncol.*, 3:76.1–76.10, 2013.

[18] H. Enderling, L. Hlatky, and P. Hahnfeldt. The tumor growth paradox and immune system mediated selection for cancer stem cells. *Bull. Math. Biol.*, 75:161–184, 2013.

[19] H. Fakir, L. Hlatky, H. Li, and R. Sachs. Repopulation of interacting tumor cells during fractionated radiotherapy: Stochastic modeling of the tumor control probability. *Medical Physics*, 40:121716.1–121716–8, 2013.

[20] A.A. Forastiere, H Goepfert, and M. et al. Maor. Concurrent chemotherapy and radiotherapy for organ preservation in advanced laryngeal cancer. *N. Engl. J. Med.*, 349:2091–2098, 2003.

[21] R. Ganguli and I.K. Puri. Mathematical model for the cancer stem cell hypothesis. *Cell Proliferation*, 39:3 – 14, 2006.

[22] J. Gong. *Tumor Control Probability Models*. PhD thesis, University of Alberta, Canada, 2011.

[23] J. Gong, M.M. dos Santos, C. Finlay, and T. Hillen. Are more complicated tumour control probability models better? *Math. Med. Biol.*, 30:1–19, 2013.

[24] P.B. Gupta, C.M. Fillmore, G. Jiang, S.D. Shapira, K. Tao, C. Kuperwasser, and E.S. Lander. Stochastic state transitions give rise to phenotypic equilibrium in populations of cancer cells. *Cell*, 146:633–644, 2011.

[25] D. Hanahan and R.A. Weinberg. The hallmarks of cancer. *Cell*, 100:57–70, 2000.

[26] T. Hillen and J.W.N. Bachmann. Mathematical optimization of the combination of radiation and differentiation therapies for cancer. *Frontiers in Oncology*, 3(52), March 2013.

[27] T. Hillen, H. Enderling, and P. Hahnfeldt. The tumor growth paradox and immune system-mediated selection for cancer stem cells. *Bulletin of Mathematical Biology*, 75:161–184, 2013.

[28] S. Hiremath, S. Sonner, C. Surulescu, and A. Zhigun. On a coupled SDE-PDE system modeling acid-mediated tumor invasion. *Discr. Cont. Dyn. Syst. B*, 23:2339–2369, 2018.

[29] S. Hiremath and C. Surulescu. A stochastic multiscale model for acid mediated cancer invasion. *Nonlinear Analysis: Real World Applications*, 22:176–205, 2015.

[30] S. Hiremath and C. Surulescu. A stochastic model featuring acid-induced gaps during tumor progression. *Nonlinearity*, 29:851–914, 2016.

[31] Y. Iwasa, M.A. Nowak, and F. Michor. Evolution of resistance during clonal expansion. *Genetics*, 172:2557–2566, 2006.

[32] A. Jackson, G.J. Kutscher, and E.D. Yorke. Probability of radiation-induced complications for normal tissues with parallel architecture subject to non-uniform irradiation. *Medical Physiscs*, 20:613–625, 1993.

[33] M. Jackson, F. Hassiotou, and A. Nowak. Glioblastoma stem-like cells: at the root of tumor recurrence and a therapeutic target. *Carcinogenesis*, 36:177–185, 2015.

[34] P. Källman, B.K. Lind, and A. Brahme. An algorithm for maximizing the probability of complication-free tumour control in radiation therapy. *Phys. Med. Biol.*, 37(4):871–890, 1992.

[35] I. Karatzas and S. Shreve. *Brownian Motion and Stochastic Calculus*. Springer, 1991.

[36] W.K. Kelly, O.A. O'Connor, L.M. Krug, J.H. Chiao, M. Heaney, T. Curley, B. MacGregore-Cortelli, W. Tong, J.P. Secrist, L. Schwartz, S. Richardson, E. Chu, S. Olgac, P.A. Marks, H. Scher, and V.M. Richon. Phase 1 study of an oral histone deacetylase inhibitor, suberoylanilide hydroxamic acid, in patients with advanced cancer. *Journal of Clinical Oncology*, 23:3923–3931, 2005.

[37] Y. Kim, K.M. Joo, J. Jin, and D.H. Nam. Cancer stem cells and their mechanism of chemo-radiation resistance. *Int. J. Stem Cells*, 2:109–114, 2009.

[38] P. Kloeden, S. Sonner, and C. Surulescu. A nonlocal sample dependence SDE-PDE system modeling proton dynamics in a tumor. *Discr. Cont. Dyn. Syst. B*, 21:2233–2254, 2016.

[39] N. Komarova and D. Wodarz. Effect of cellular quiescence on the success of targeted CML therapy. *PLoS ONE*, 2:e990.1–e990.9, 2007.

[40] J. Kroos. An SDE approach to cancer therapy including stem cells, 2014. Master thesis, University of Münster.

[41] G.J. Kutscher and C. Burman. Calculation of complication probability factors for non-uniform normal tissue irradiation: The effective volume method. *Int. J. Rad. Oncol. Biol. Phys.*, 16:1623–1630, 1989.

[42] K. Leder, E.C. Holland, and F. Michor. The therapeutic implications of plasticity of the cancer stem cell phenotype. *PLoS ONE*, 5:e1436, 2010.

[43] J.T. Lymann. Complication probability as assessed from dose-volume histograms. *Radiation Research*, 104(2):13–19, November 1985.

[44] C. Maenhaut, J.E. Dumont, P.P. Roger, and W.C.G. van Staveren. Cancer stem cells: a reality, a myth, a fuzzy concept or a misnomer? an analysis. *Carcinogenesis*, 31(2):149–158, 2009.

[45] S. Matsuda, T. Yan, A. Mizutani, T. Sota, and Y. et al. Hiramoto. Cancer stem cells maintain a hierarchy of differentiation by creating their niche. *Int. J. Cancer*, 135:2736, 2014.

[46] P. Munoz, M.S. Iliou, and M. Esteller. Epigenetic alterations involved in cancer stem cell reprogramming. *Molecular Oncology*, 620-636:6, 2012.

[47] N. Navin, J. Kendall, J. Troge, and P. et al. Andrews. Tumour evolution inferred by single-cell sequencing. *Nature*, 472:90 – 94, 2011.

[48] A. Niemierko and M. Goitein. Modeling of normal tissue response to radiation: the critical volume model. *Int. J. Rad. Onc. Biol. Phys.*, 25:135–145, 1993.

[49] A. Oroji, M. Omer, and S. Yarahmadian. An Itô stochastic differential equations model for the dynamics of the MCF-7 breast cancer cell line treated by radiotherapy. *J. Theor. Biol.*, 21:128–137, 2016.

[50] F. Pajonk, E. Vlashi, and W.H. McBride. Radiation resistance of cancer stem cells: The 4 R's of radiobiology revisited. *Stem Cells*, 28(4):639–648, 2010.

[51] G.A. Pavliotis. *Stochastic Processes and Applications. Diffusion Processes, the Fokker-Planck and Langevin Equations*. Springer, 2014.

[52] P.R. Pazdziorek. Mathematical model of stem cell differentiation and tissue regeneration with stochastic noise. *Bull. Math. Biol.*, 76:1642–1669, 2014.

[53] G. Powathil, M. Kohandel, S. Sivaloganathan, A. Oza, and M. Milosevic. Mathematical model of brain tumors: effects of radiotherapy and chemotherapy. *Physics in Medicine and Biology*, 52:3291–3306, 2007.

[54] X.S. Qi, C.J. Schultz, and X.A. Li. An estimation of radiobiologic parameters from clinical outcomes for radiation treatment planning of brain tumor. *Int. J. Radiat. Oncol. Biol. Phys.*, 64:1570–1580, 2006.

[55] P. Rajan and R. Srinivasan. Targeting cancer stem cells in cancer prevention and therapy. *Stem Cell Rev.*, 4:211–216, 2008.

[56] G. Rosenkranz. Growth models with stochastic differential equations. An example from tumor immunology. *Math. Biosci.*, 75:175–186, 1985.

[57] L. Salvatori, F. Caporuscio, Verdina A., G. Starace, and S. et al. Crispi. Cell-to-cell signaling influences the fate of prostate cancer stem cells and their potential to generate more aggressive tumors. *PLoS ONE*, 7:e31467.1–e31467.14, 2012.

[58] M. Sehl, H. Zhou, J.S. Sinsheimer, and K.L. Lange. Extinction models for cancer stem cell therapy. *Math. Biosci.*, 234:132–146, 2011.

[59] S. Selvin. *Survival Analysis for Epidemiologic and Medical Research. A Practical Guide*. Cambridge Univ. Press, 2008.

[60] Y. Shiozawa, B. Nie, K.J. Pienta, T.M. Morgan, and R.S. Taichman. Cancer stem cells and their role in metastasis. *Pharmacology & Therapeutics*, 138:285–293, 2013.

[61] A.V. Skorohod. *Studies in the Theory of Random Processes*. Addison-Wesley Publ. Company, 1965.

[62] A.L. Stensjøen, O. Solheim, K.A. Kvistad, A.K. Håberg, Ø. Salvesen, and E.M. Berntsen. Growth dynamics of untreated glioblastomas in vivo. *Neuro Oncol.*, 17:1402–1411, 2015.

[63] T. Stiehl and A. Marciniak-Czochra. Mathematical modeling of leukemogenesis and cancer stem cell dynamics. *Mat. Model. Nat. Phenom.*, 7:166 – 202, 2012.

[64] T. Stocks, T. Hillen, J. Gong, and M. Burger. A stochastic model for the normal tissue complication probability (NTCP) and applications. *Math. Med. Biol.*, 34:469–492, 2017.

[65] C. Surulescu and N. Surulescu. Some classes of stochastic differential equations as an alternative modeling approach to biomedical problems. In P. Kloeden and C. Pötzsche, editors, *Nonautonomous Dynamical Systems in the Life Sciences, LNM 2102*, pages 269–307. Springer, 2013.

[66] B.T. Tan, C.Y. Park, L.E. Ailles, and I.L. Weissman. The cancer stem cell hypothesis: a work in progress. *Lab. Invest.*, 86:1203–1207, 2006.

[67] C.M. van Leeuwen, A.L. Oei, J. Crezee, A. Bel, N.A.P. Franken, L.J.A. Stalpers, and H.P. Kok. The alfa and beta of tumours: a review of parameters of the linear-quadratic model, derived from clinical radiotherapy studies. *Radiation Oncology*, 13:96, 2018.

[68] H. Youssefpour, X. Li, A.D. Lander, and J.S. Lowengrub. Multispecies model of cell lineages and feedback control in solid tumors. *Journal of Theoretical Biology*, 304:39–59, 2012.

[69] M. Zaider and G.N. Minerbo. Tumor control probability: a formulation applicable to any temporal protocol of dose delivery. *Phys. Math. Biol.*, 45:279–293, 2000.